

Dear Editor,

Please find below our replies to the referees' comments and a revised manuscript that incorporates changes based on the feedback received.

The main change to the manuscript is the inclusion of an expanded discussion about the relationship between the porous anisotropy we observe in our experiments and the mechanics of mylonites. Referee 1 found that there was a logical gap in our previous text when it came to how and when the pore sheets would have a mechanical impact. This was echoed by several questions and comments from Referee 2. We agreed with the referees' perspectives and have provided a larger discussion. We kindly thank the referees for their constructive comments and hope that they find our expanded discussion is a more complete treatment.

Minor changes include a new figure (formerly fig. 3g) and some clarifications over what we are suggesting to be reappraised. In the initial submission we think that we worded some sentences poorly and gave the wrong impression about what our opinions were in relation to the constitutive models of irreversible physical deformation in rocks. Additionally, some of the consequences of including creep cavities in the general shear zone model that were formerly included within the text (and a few more examples) have now been given their own section. We have also relabelled the minerals in the new figure after some new analysis conducted since the initial submission (we have now included this in the appendix).

We have attempted to remain in keeping with the nature of a short communication and we hope that you feel that the revised manuscript achieves this while addressing the referees' concerns.

Best wishes,

James Gilgannon

#####

In the following, referee comments are in grey and responses are in black.

Please find a copy of the manuscript with changes marked below the replies.

#####

Response to the comments of Alberto Ceccato (Referee 1):

Lines 13–14: please add some references supporting this statement.

Some example references have now been added.

Lines 32–34: I partially disagree with these two sentences. It is true that much of the past advances on the creep cavitation subject results from experimental works and micro-scale analysis (as the cited references report); but it is also true that many other authors have evaluated the extension and occurrence of creep cavitation and related phenomena in natural polymineralic shear zones deformed at geological conditions and have tried to qualitatively extrapolate their results from the thin section-scale to crustal-scale shear zones (e.g. Giuntoli et al., 2020 SciRep <https://doi.org/10.1038/s41598-020-66640-3>; Preciguet et al., 2017 NatComm <https://doi.org/10.1038/ncomms15736>).

We have changed the text accordingly to reflect this and it now points the reader to a few other examples.

I understand that your samples are “natural” geo-materials, but you are presenting the results of experimental deformation at lab conditions, not geological conditions. I suggest the Authors to recast these two sentences taking into consideration this observation. I would focus on two main points that, in my opinion, are the strong points and the novelty of the paper: 1) the quantitative approach to evaluate the extension of creep cavitation processes; 2) the occurrence of creep cavitation in monomineralic shear zone.

This is an excellent point and we agree that the experiential conditions of any laboratory deformation places limits on the interpretation of the results obtained. However, in principle the model of Fusseis et al. (2009) is a Generalised Thermodynamical model that is driven by the coupling of specific dissipative length scales that leads to an entropic steady state and therefore can, to an extent, be tested outwith of ‘natural’ deformation conditions. To do this we use these experiments as windows on an entropic steady state with the caveat that the processes activate are comparable to those that would activate in nature.

So, while it was never quantified in the original experiments, the experiments of Barnhoorn et al. (2004) are taken to qualitatively meet this thermodynamic requirement of steady state: that is the system underwent adjustment to accommodate the imposed deformational work and attained a mechanical and microstructural steady state. As the dissipative processes observed in the microstructure are similar to those seen in nature (e.g. creep accomplished by the migration of dislocations, sub-grain rotation

recrystallisation) it can be assumed that, despite the higher rate of work being done, the experimental boundary conditions keep the rock in a window that is still representative of how the rock sample could dissipate deformational energy at mid-crustal conditions when the system was closed. In this way, we are testing aspects of the Generalised Thermodynamic hypothesis of Fusses et al. (2009) and do not find the difference in experimental conditions to nature as problematic as it may seem at a first pass. For this reason we have retained our original formulation as we wished to focus on the physical predictions and physical models.

Line 40: please, specify what you have revisited of the set of classical experiments (the microstructures of the deformed samples).

We have changed the text accordingly.

Line 55: please, specify if you have considered these grain-filled pores as “porosity” during the following density quantification or not. I guess you have considered it as “porosity”, but this is not clear neither from the main text, nor from the Method section (or perhaps I missed it).

In the quantification only open pore space is mapped. There will be some pores that are partially filled with a precipitate but it is only the open space that is segmented and counts towards the porosity. We have clarified the text in the segmentation and wavelet analysis sections of the appendix accordingly.

Line 89: I would replace “microstructure of . . .” with “the spatial arrangement of syn-kinematic pores”. In my opinion, the definition of the effective microstructure would imply the analysis and characterization of pore typology, connection, morphology, etc. . .

We have changed the text accordingly.

Line 94: Even though I agree with the Authors about the importance of the spontaneous development of a systematic pore pattern, this statement is rather speculative and not fully supported by the data presented in the manuscript. “Bulk material properties” is rather generic and vague. What are these bulk material properties and initial heterogeneities? Grain size? Mono-polymineralic composition of the sample? (What about the experimental boundary conditions? Shear strain rate? confining pressure? Sample/Room humidity and fluid availability?) I understand that this could lead to further discussion that goes beyond the scope of this short communication, but I would like the Authors to be a little bit more specific on the term “bulk material properties” if they want to keep the sentence. On the other hand, if the Author want to work around this

comment: highlight the lack of any initial heterogeneity and state that, at present, the genetic causes of this microstructure need further investigations. . .

Thank you for pointing this out, we agree that it is not clear as to what we were trying to express. We have changed the text to be less ambiguous and reflect the referee's suggestion. However, we would like to refrain from expounding on exactly which material property could be responsible. Our data does not allow us to say more than the observation of a porous anisotropy seems to be relevant to the sample scale (ie millimetres). With regards to what we consider material properties and heterogeneities we have provided some examples in the text but consider the wide spread definitions of what these are generically in the geological textbooks (e.g. Twiss and Moores, 2007; Fossen, 2010) to be something that we do not need to define in the manuscript. For the purposes of this reply we will say that we consider a material property to be an intrinsic property of the bulk material that is used in a macroscopic description of deformation. Furthermore, it is intensive and does not depend on the amount of the material. Scalar descriptions of microstructural features, like an average grain-size, we consider to be structural properties that describe the state of the material (cf. Kocks et al., 1975). As structural properties generally vary through the rock they can be one source of the kinds of initial heterogeneities that we refer to.

Twiss, R.J., & Moores, E.M. (2007). Structural geology. New York, NY, W.H. Freeman.

Fossen, H. (2010). Structural geology. Cambridge, Cambridge University Press.

Kocks, U., Argon, A., and Ashby, M.: Thermodynamics and kinetics of slip, vol. 19 of Progress in Materials Science, Pergamon Press Ltd, 1975.

Lines 104–106: These two sentences are rather speculative and vague. Unfortunately, it seems to me that a logical connection between the occurrence of strain invariant mechanical parameters and the possible evolution of pore sheets into creep fractures is missing. In my opinion, this paragraph suffers from two main problems: (1) there are no direct logical links between the observation of strain invariant mechanical parameters and the evolution of pore sheets into creep fractures, i.e. the maintenance of strain invariant mechanical parameters is not a sufficient conditions to prove (or just speculate) that also your pore sheets will evolve into creep fractures. (2) Even though the experiments of Dimanov et al. and Rybacki et al. have been performed under similar conditions to those reported here, there are some fundamental differences that might undermine your inference: a) different lithologies; b) occurrence of creep fractures at relatively low strains if compared to shear strains obtained in Barnhoorn et al.; c) lack of any evidence of creep

fractures in the set of experiments of Barnhoorn et al. (2004). Rather than a speculation on the possible evolution of these pore sheets under “variable” natural conditions, I would suggest the Authors to discuss and compare in a more detailed manner their experimental results and inferences with those presented by Dimanov et al (2007) and Rybacki et al. (2008). Then, a speculative extrapolation to the natural conditions might be attempted. Indeed, there might be some microstructural similarities between the cited references and the data reported in the manuscript that might better support your speculation about the “possible evolution of pore sheets into creep fractures”. In addition, “natural conditions are more varied” is a rather vague and generic statement. What are these variable natural conditions? Transient shear strain rates? Wet vs. dry conditions? Please specify if you want to keep the sentence.

We agree with the referee’s perspective (which is mirrored in the comments of Referee 2) and have substantially changed the discussion about pore sheets and the mechanics of mylonites.

We now provide a discussion on how the effect of boundary conditions, a more comprehensive note of the differences and similarities of those comparable experiments and others (Dimanov et al. (2007), Rybacki et al. (2008), Rybacki et al. (2010) and Delle Piane et al. (2008)). While still done in a speculative way, we now discuss some natural conditions more precisely. In general we have kept the same argument but have added some of the logic that had brought us to our initially more brief paragraph about the mechanics of shear zones and how pore sheets could impact on this.

Rybacki, E., Wirth, R. and Dresen, G., 2010. Superplasticity and ductile fracture of synthetic feldspar deformed to large strain. *Journal of Geophysical Research: Solid Earth*, 115(B8).

Delle Piane, C., Burlini, L., Kunze, K., Brack, P. and Burg, J.P., 2008. Rheology of dolomite: Large strain torsion experiments and natural examples. *Journal of Structural Geology*, 30(6), pp.767-776.

Technical Corrections:

Figure 1: please, enhance the brightness/contrast of the BSE images OR enlarge the images (this might help the reader to instantaneously capture the porosity distribution even if the image is very small).

We have enhanced the image to better show the contrast between features. We have also made a new figure (formerly fig. 3g) that shows the detail of a pore sheet. We would rather not change the scale of figure 1's panels as part of what we wish to emphasise is that the porosity is a feature that is relevant at the sample scale and is not just a local phenomenon.

Figures in the supplement: There is a discrepancy between the figure call-out in the text (Figure S*) and the Figure captions (Figure A*). Please change one or the other to be consistent throughout the text.

Thank you for pointing this out, we have changed the text to reflect the figure captions.

Line 245: There's probably a reference typo [(18) ???].

It was, thank you, we have changed it to the correct reference.

#####

Response to the comments of Lars Hansen (Referee 2):

-The nature of the cavities:

My question in this context is whether or not there is a pore fluid, and if so, what is its composition? One item of concern is whether the pores are filled with CO₂. That is, could there be some decarbonation of the calcite during initial pressurization and heating that generates porosity? Caristan, Harpin, and Evans (1981) presented evidence of calcite decarbonization during hot-pressing of calcite aggregates in a gas- medium apparatus, and it seems worth discussing whether or not something similar has occurred here. This question could be answered in some part by comparing the starting material (not shown) to the low-strain material ($\gamma = 0.4$).

We have amended part of the text in discussion section 3.1 to include some inferences about the possible composition of the fluid, which we agree likely has CO₂ as a component. It would, of course, be more satisfying to know the exact composition of the fluid that filled the pores, but this is beyond the scope of our study and we feel that the impact and importance of the new results presented is not undermined by a lack of knowledge of the fluid composition.

Regarding the straight forward calcite decarbonation reaction, which we do not address in the text directly, we think that it is likely not occurring as it is not thermodynamical favourable for the deformation conditions (e.g. Ivanov and Deutsch, 2002; Shatskiy et al., 2018). However it is very likely that the minor amounts of dolomite present in the Carrara

marble samples will allow a release of CO₂ through the reaction Dol \leftrightarrow Cc + Per + CO₂ (cf. Delle Piane et al., 2008).

Ivanov, B.A. and Deutsch, A., 2002. The phase diagram of CaCO₃ in relation to shock compression and decomposition. *Physics of the Earth and Planetary Interiors*, 129(1-2), pp.131-143.

Shatskiy, A., Podborodnikov, I.V., Arefiev, A.V., Minin, D.A., Chanyshv, A.D. and Litasov, K.D., 2018. Revision of the CaCO₃–MgCO₃ phase diagram at 3 and 6 GPa. *American Mineralogist: Journal of Earth and Planetary Materials*, 103(3), pp.441-452.

Delle Piane, C., Burlini, L., Kunze, K., Brack, P. and Burg, J.P., 2008. Rheology of dolomite: Large strain torsion experiments and natural examples. *Journal of Structural Geology*, 30(6), pp.767-776.

–The evolution of porosity and its measurement:

Considering that some porosity may be present at the onset of deformation, the fundamental question is whether or not the porosity increases with deformation. A primary conclusion of the previous work (Gilgannon et al., GRL, 2020), which analyzes one of the same samples as in this paper (PO422, gamma = 5), is that porosity increases due to pore nucleation associated with recrystallization. Indeed, the previous work presents excellent observations of pores associated with new grain boundaries, and a total porosity of ~1%, but as far as I can tell, it is never demonstrated that deformation increases the total porosity.

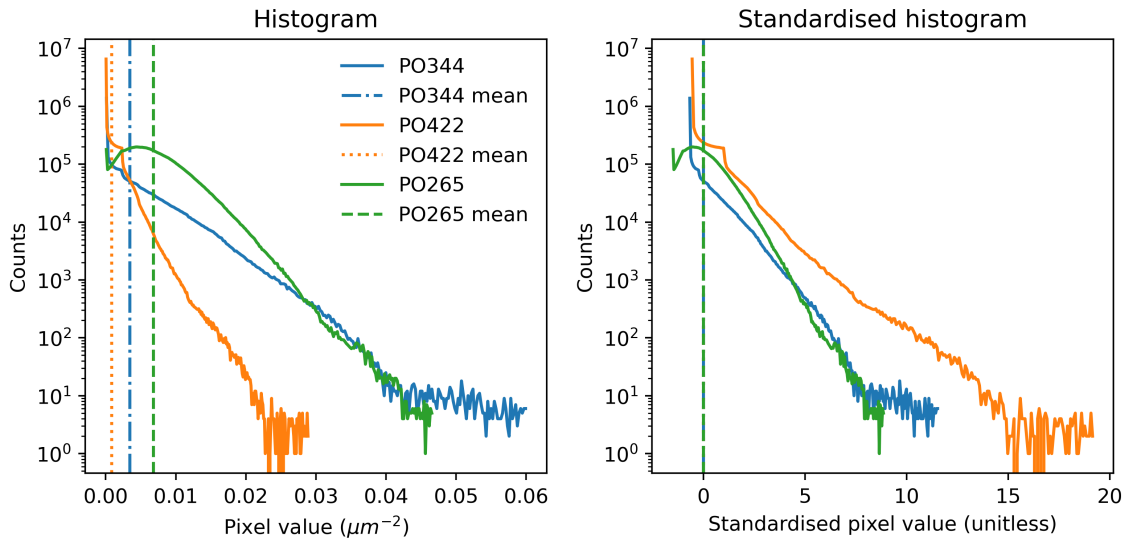
The present work presents an excellent opportunity to make that demonstration since samples deformed to a variety of strains are analyzed. However, it is still not clear to me that there is a change in the total porosity. The wavelet analysis definitely demonstrates a change in the spatial distribution of pores, but as far as I understand, it does not present an increase in the porosity.

My conclusion here stems from the details of the measurement of porosity density, which is the fundamental measurement presented in the paper. As I understand the measurement procedure described in the appendix, only the centroids of identified pores are used in the construction of the porosity density maps. Thus, “porosity density” is apparently the number of pores per unit area, and this quantity may be better referred to as the “pore density”. I admit I had some confusion about how “standardized density” is defined, why it is unitless, and why it can have negative values. Some clarification here would be valuable in a revised version, but for now it seems to me to represent a

normalized version of the “pore density” and not the porosity (pore volume per total volume).

We thank the referee for the feedback and we agree that pore density is a more correct way to refer to the quantity and have changed the text and figures accordingly.

To the point of the standardised, and unitless, density: this occurs through the implementation of equation A7 where the value of each pixel is divided by the standard deviation of the image which has the same units as the pixel values of the image. We do this for the purposes of standardising the histograms of each pore density raster. This is because the wavelet analysis benefits from analysis on a field that has a mean value of zero (see reply fig. 1 below) and is an advised step for the correct use of the wavelet convolution.



Reply fig. 1: The histograms for both the raw and standardised values of the various kernel density density maps.

We must doubly thank the referee: because of his question we realised that we had mistakenly not retained the floating point information on the rasters and our calculations had been made on greyscale values rather than the correct density units. This did not affect our results, as it was simply a transformation of the values in the density field, but we recalculated each step of the wavelet analysis to be sure and our figures now present this correct data: there was no change in the results. We now use arrows in the visualisation of the pore density figures to show that the colour bar is clipped and other higher and lower values exist.

To the point of whether or not porosity increases: in the initial submission of the text we only referred to the spatial extent of the porosity (which does increase) and avoided discussing if the absolute porosity changed at all. The absolute porosity does in fact increase and based on the referee's desire to know this information we have chosen to now include it (now reported in the new table 1 of the manuscript).

We were reluctant to include this in the initial submission because image segmentation has many hard-to-account-for uncertainties and because there may have been grain boundaries included within our particular choice of workflow. After some consideration we are only willing to include these values because we note that the change in porosity between gamma 5 and 10.6 is on an order of magnitude. As the seed based segmentation (randomwalker) algorithm used the same diffusion gradient and dark seed value for each image it is likely that this change of an order of magnitude is real. Additionally as the pore shape filter used is the same between data sets and the pore shapes are not expected to change significantly between strains we expect that we are comparing comparable pore populations and hence syn-kinematic porosity values.

Unfortunately, the "pore density" does not seem as valuable as porosity in regards to interpreting the hydromechanical effects of the observed microstructural evolution. A key inference in the paper is that permeability is enhanced (and becomes anisotropic) during deformation. The relationship between permeability and porosity is not trivial, but if the porosity were known, a back of the envelope calculation could be made to assess the potential changes in permeability expected. However, I don't think changes in permeability can be assessed qualitatively or quantitatively when using only the number of pores. Furthermore, from the data presented here, it seems entirely possible that the porosity could be constant with increasing deformation, even though the number and distribution of discrete pores evolves.

As our paper seeks to test aspects the dynamic granular fluid pump model (Fusseis et al., 2009; Regnenauer-Lieb et al., 2009) and hence discuss the results in this context, it is not possible to calculate the permeability expected to be produced by the pump simply from porosity values. This is because the permeability is time dependent and a result of both mechanical and chemical dissipation. This makes the kind of back-of-the-envelope calculation for permeability not possible. In this sense one has to solve a full system of coupled non-linear equations to make a prediction of what the permeability is in the model of the dynamic granular fluid pump model. The strength of our results is that they observationally validate some of the predictions of the model of Fusseis et al. (2009) and provide the first unambiguous evidence in favour of the well cited but little tested dynamic

granular fluid pump model. We agree that it would be of interest for future work to attempt such a calculation and model the consequences of the increase in porosity and its extent.

Regenauer-Lieb, K., Yuen, D.A. and Fousseis, F., 2009. Landslides, ice quakes, earthquakes: a thermodynamic approach to surface instabilities. In *Mechanics, Structure and Evolution of Fault Zones* (pp. 1885-1908). Birkhäuser Basel.

As a final note on this topic, there is a clear link to previous work on the segregation of melt during deformation of partially molten rocks (for a review, see Kohlstedt and Holtzman, AREPS, 2009). I'm surprised to not see any of that work referenced in the present manuscript. Those studies demonstrate that the (melt-filled) porosity can dynamically arrange into planar features not dissimilar to the "periodic pore sheets" described here. However, I'll emphasize that the average porosity is static in those experiments. Locally it may increase or decrease, some new pores are created, some old ones are destroyed, but the total porosity does not change. It remains to be demonstrated that a similar phenomenon is not occurring in the calcite samples analyzed here and that the overall porosity is actually increasing.

We agree that there is a strong connection to the topic but we have refrained from a discussion in this direction for two reasons: (1) other work has tackled this exact comparison (Spiess et al., 2012) and (2) our experiments are considered to reflect the behaviour of single phase aggregates. There is much to discuss when considering only the implications for sub-solidus deformation in single phase aggregates and any more discussion about how the system would behave with melts would not let us keep to the short communication format we have submitted. We hope that other future contributions by the community will pick up on the work already started by Spiess et al., (2012) in considering the role of creep cavities and melt segregation.

Spiess, R., Dibona, R., Rybacki, E., Wirth, R. and Dresen, G., 2012. Depressurized cavities within high-strain shear zones: their role in the segregation and flow of SiO₂-rich melt in feldspar-dominated rocks. *Journal of Petrology*, 53(9), pp.1767-1776.

–Challenging the concept of rocks as viscous fluid:

The authors take the discussion beyond the development of a periodic array of pores to comment on whether or not rocks can be treated as viscous fluids. The paper is framed around the common treatment of rocks as viscous fluids at long timescales and suggests that that framework is flawed and a new paradigm involving creep cavitation is necessary. Emphasis is given to the transition from viscous to brittle behavior.

I suggest that these statements are overstating the case and detract from what is otherwise a useful paper about applying wavelet analysis to periodic pore distributions. My primary concern here is that the authors do not provide any evidence that the mechanical properties of the rocks investigated are modified by the formation of an anisotropic pore distribution. The mechanical data have already been published in previous work, so if these pore sheets are significant to the rheological behavior, then the authors can demonstrate that with the mechanical data. Furthermore, if these rocks can't be described as viscous fluids because of the porosity evolution, then the authors could again demonstrate that with the mechanical data.

In addition, I'll note that viscosity is a phenomenological description, and when discussed in the context of crystalline materials, is generally only taken to apply at macroscopic scales. For example, we often discuss rocks as fluids with non-Newtonian viscosities for which the viscosity is controlled by the dynamics of dislocations at the lattice scale. There has been much work in the materials sciences over the past several decades demonstrating that, at scales well below the grain size, dislocation propagation occurs in discrete bursts (key terms are "dislocation avalanches" and "jerky flow"). This behavior is clearly not viscous, but when averaged over many crystals of many orientations, the mechanical behavior can still be described as viscous.

Key to the authors' argument is that creep cavitation can lead to brittle behavior, which "can never be predicted by flow laws commonly used to model viscous deformation." An analogous case can be seen in the fatigue of metals. Constitutive equations have existed for some time to describe plastic deformation (i.e., having a yield stress and strain hardening) in metals. Similarly, the equations of plasticity cannot describe failure in fatigue. Does that mean that metals do not deform plastically? Does that mean that we need a new paradigm and must throw out constitutive descriptions of plasticity? I think the answer to both questions is "no" since, although we need additional physics to describe fatigue, there are many situations in which a plastic description of metals is totally appropriate. Similarly, I'd argue that there are many situations in which the description of rocks as viscous fluids is totally appropriate.

So, at the very least, I suggest the authors weaken their comments to note that rocks can reasonably be treated as viscous fluids in many situations.

As a final note, although the formation of pore sheets may require additional physics in our constitutive models, in many cases, these additional physics can be described as an evolving viscosity. A relevant example is the work of Holtzman, King, and Kohlstedt

(EPSL, 2012), who present a framework for describing the evolution of the viscosity of partially molten rocks as planar features of high porosity are formed.

We think that we have worded some sentences poorly in the original submission and have given the wrong impression to the referee: our argument was not intended to claim that viscosity as a constitutive model is wrong. We have reworded text where we can to make this clearer. Our discussion that pertains to pore sheets and mechanics is significantly longer now and hopefully clearer. We have tried to fill in the logical gaps noted by Referee 1 and 2 in the original section of the text. Largely, our argument points to the same messages but we hope that the longer discussion helps the reader follow the argument more easily now.

The fact that a mylonite deforms in a fashion that can be described with a viscous model is something we agree with. Moreover we have no problem with any constitutive model. We wished to argue the case for the Generalised Thermodynamic model behind the work of Fousseis et al. (2009). We can see how the very short discussion in our initial submission coupled with some imprecise wording lead the referee towards his point.

In the Generalised Thermodynamic model behind the work of Fousseis et al. (2009) a mechanical rate equation is essential but it is not sufficient to fully describe mechanical dissipation. That is to say that we wished to open a discussion in the community about a perspective that does not limit a mylonite to solely slow aseismic creep. The strength of our work is that it shows there is some validity to at least one of the predictions of the dynamic granular fluid pump model (Fousseis et al., 2009). We wished to argue that the fact we found what is otherwise unexpected in our current perspective of shear zones warrants discussion. This is especially true when there is another perspective, that of the dynamic granular fluid pump model, that predicts the observation should be there. Moreover, it is even more pertinent when a range of experiments show similar results.

Our contribution hopes to showcase the fact that quantitative testing validates parts of a paradigm that has consequences far beyond an esoteric porosity. Additionally, we fully agree with the concept of scales of deformation and the need for homogenisation of processes when considering their dissipative effects: this is explicitly part of the framework that makes up the Generalised Thermodynamic model we are arguing favourably for (cf. Regenauer-Lieb et al., 2013; Regenauer-Lieb et al., 2014; Veveakis and Regenauer-Lieb, 2014). We hope that our chief aim, that of arguing for the Generalised Thermodynamic paradigm concerning creep cavities, is clearer now in the text and the expanded discussion.

Regenauer-Lieb, K., Veveakis, M., Poulet, T., Wellmann, F., Karrech, A., Liu, J., Hauser, J., Schrank, C., Gaede, O. and Trefry, M., 2013. Multiscale coupling and multiphysics approaches in earth sciences: Theory. *Journal of Coupled Systems and Multiscale Dynamics*, 1(1), pp.49-73.

Regenauer-Lieb, K., Karrech, A., Chua, H.T., Poulet, T., Veveakis, M., Wellmann, F., Liu, J., Schrank, C., Gaede, O., Trefry, M.G. and Ord, A., 2014. Entropic bounds for multi-scale and multi-physics coupling in earth sciences. In *Beyond the Second Law* (pp. 323-335). Springer, Berlin, Heidelberg.

Veveakis, E. and Regenauer-Lieb, K., 2015. Review of extremum postulates. *Current Opinion in Chemical Engineering*, 7, pp.40-46.

–Minor comments:

Line 20: It's not clear to me that the term "frictional embrittlement" is appropriate here. Is the implication that friction leads to brittle deformation, in the manner that hydrogen embrittlement means hydrogen doping leads to brittle behavior? I have been unable to find another use of this term in the literature.

We have changed the text to remove this phrasing. It now reads:

It is this fracturing, which can have physical (e.g. Beall et al., 2019) or chemical (e.g. Alevizos et al., 2014) driving forces, that creates seismicity and mass transport pathways through the deep Earth (Sibson, 1994).

Line 23: This does not seem like an appropriate reference here. The book by Kocks, Argon, and Ashby is certainly a classic work, but it is primarily focused on the small-scale aspects of dislocation motion. Their treatise is focused on the mechanisms that lead to plastic deformation (as in deformation with a yield stress), and I don't think they refer to geological processes, viscous behavior, or creep.

We agree that, while it does treat homogenised macroscopic deformation, the work of Kocks et al. (1975) is not the most geologically relevant citation. Therefore, we have changed the reference here to two more geologically relevant references:

Hobbs, B. and Ord, A.: *Structural Geology: The Mechanics of Deforming Metamorphic Rocks*, Elsevier, Netherlands, 2015.

Poirier, J.-P.: *Creep of Crystals: High-Temperature Deformation Processes in Metals, Ceramics and Minerals*, Cambridge Earth Science Series, Cambridge University Press, <https://doi.org/10.1017/CBO9780511564451>, 1985.

Line 25: It seems strange to refer to these rocks as viscous when the primary argument of the paper is that we can't think of rocks as viscous.

As discussed above, we apologise for the confusion but our primary argument was not to we cannot think of rocks as viscous. The text now reads:

While much of this paradigm remains to be tested, the notion that mylonites generate self-sustaining and dynamic pathways for mass transport is radical and consequential for the interpretation of how deep shear zones behave during deformation.

Line 35: The authors state here that the evidence is unambiguous for the role of creep cavities. This phrasing seems a bit strong to me considering my main comments above.

We have changed this part of the introduction and it now reads as:

In this contribution we provide unambiguous experimental evidence in a natural starting material that supports, and extends, the paradigm concerning the role of creep cavities in shear zones. We present quantitative results showing that creep cavities are a spatially significant feature of viscous deformation, being generated in periodic sheets throughout the samples. Our analyses are intentionally made over large areas of the experimentally deformed samples in order to contextualise and understand the role of creep cavities at a scale more comparable to those where macroscopic material descriptions are unusually made. We argue that our results warrant a reappraisal of the community's perception of how viscous deformation proceeds with time in rocks and suggest that the general model for viscous shear zones should be updated to include creep cavitation. A key consequence of this would be that the energetics of the deforming system become the keystone of our perspective rather than the mechanics.

Line 54: At this point in the text, I was looking for a description of the sample preparation and data collection procedures. I eventually found a lot of this in the Appendix, but I think this part of the main text should point the reader to the relevant sections of the Appendix.

We have added direction for the reader to find the methods now in section 2 of the manuscript.

Figure 1: It would be very useful to know what the starting material looks like. In other words, does the porosity evolve simply as a function of increasing the confining pressure and temperature?

Unfortunately we did not have access to the starting material. We consider the reference of a sample that has not experienced dynamic recrystallisation as adequate for the argument we wished to make.

Figure 1: It would also be useful to state in the caption how the images were collected (e.g., BSE images in SEM).

We have altered the figure caption to include this information.

Line 55: I'm curious how the authors distinguish between a pre-existing second phase and a new precipitate. And on a related note, if some pores are filled with precipitates, then are they still considered pores in this analysis? Based on the text here and in the appendix, it is unclear to me if, and if so how, secondary phases are removed from the porosity density maps.

We have changed the text in the methods section to reflect that we only segment open porosity.

Regarding the nature of new vs old second phases, we consider the fact that precipitates exist at the triple junctions of newly recrystallised calcite grains as a strong argument. Additionally, the precipitates often possess complex shapes that reflect the pore geometry is another strong argument. Please refer to the supplementary material of Gilgannon et al. (2020) (GRL) for a more complete argumentation of this point.

Figure 2: How come a similar analysis for the low-strain material isn't shown? That would be a useful comparison.

As we were interested in analysing the pore sheets, of which there were none before dynamic recrystallisation, the analysis does not include the low strain sample.

Figure 2: It took me a while to figure out that eta is a sort of measure of the total power for the whole map. It would be helpful to clarify this in the main text and point the reader to section A7.

We have altered the figure caption to include this information.

Figure 2: Both panels b and c have three peaks labeled, but only two are discussed in the text.

We have added text to the figure caption to explain why we do not discuss it. It reads:

We note that two local extremes are not discussed in the text. This is because one was at the sensible limit of the analysis ($\theta = -12^\circ$, $\lambda = 530 \mu\text{m}$) defined in appendix section A6 and the other did not correlate with any microstructural features ($\theta = -84.00^\circ$, $\lambda = 173 \mu\text{m}$).

Lines 73 and 74: The values given for the locations of the peaks seem too precise to me considering the broadness of the peaks. I suggest reducing the precision by at least one significant digit. Or present some measurement of error for these numbers.

We have now reduced the precision in the text to 2 significant figures.

Figure 3: Panel g seemed out of place to me here as it doesn't really have to do with the wavelet visualization. Isn't it better suited to Figure 1?

We have now made panel g its own figure.

Figure 3: It took me a while to figure out how exactly the visualizations were made. Much of this information is in the appendix, but more detail can be given here. The caption can simply state that these images represent the convolution of the density map and the wavelet, or something along those lines.

The figure caption has been changed accordingly

Line 83: The authors state here a key thrust of the paper, that the development of anisotropic porosity is not accounted for in our conceptual models. But the question that arises to me as I read this line is...do we need to account for it? I think that need is what remains to be demonstrated. Is the permeability measurably affected? Is the mechanical behavior affected? The mechanical data were collected and published for these experiments. Is there in signature in those data of the porosity evolution?

We agree that this is worth discussing and we have now substantially expanded the section pertaining to the mechanics to better treat this point.

Line 87: If an attempt is made in a future revision to quantitatively relate the observed porosity to permeability, then this seems like a good spot for a back-of-the-envelope calculation.

As discussed above, a back of the envelope calculation is not possible for the dynamic permeability in the dynamic granular fluid pump model which we test.

Line 113: The text states that "...the hydro-mechanical anisotropy presented here would...". However, hydromechanical anisotropy is not presented here. Microstructural anisotropy is presented, and the hydro-mechanical anisotropy is only inferred.

We agree and have changed the text accordingly.

Line 138: Again, how does the algorithm deal with secondary phases? Are they initially marked as pores?

We only analyse open porosity and as this has a different grey scale seed value the segmentation does not include second phases. We have changed the text to make it clearer that we only segmented and analysed open pore space.

Line 138: Here and elsewhere "S" is used instead of "A" to indicate items in the appendix.

Thank you for highlighting this. We have changed all instances of this mislabelling.

Line 161: There is a typo of some sort in this sentence.

We have changed the sentence accordingly.

Line 185: There is some explanation here, but the choice of L still seems pretty subjective. Isn't it simpler to just retry the analysis with different values of L and see how that affects the results?

Yes, as discussed in the appendix, it is convention when using wavelet analysis to choose a wavelet form that resembles the feature you are interested in. One could run the analysis through many iterations of the convolution with different kernels but this is very computationally costly. Currently we compute 60 scales and 181 orientations per pixel in the image and this requires a lot of memory. Future work may implement an automatic step to move through different kernels but it was not needed for our current purposes.

Line 215: I'm a little confused about the definition of "mean power spectrum". Is this the mean of the power spectrum? The mean of several power spectra?

We adopt the language used in the text of Torrence and Compo (1998). As we understand it, the mean power spectrum (P_k) is meant to be the mean value for the distribution of noise that would occur at a given frequency of the null model we use. In our case we use a white noise model (in which noise has the same power across frequencies). So the simplifying assumption of Torrence and Compo (1998) is that one does not have to

consider the distribution of noise at a given frequency but only what its mean value would be (P_k).

Section A6 and Figure A4: I think this is a useful analysis of the edge effects. Some aspects of this analysis could be highlighted in the main text. For instance, in Figure 3, the caption could note that the white space around the visualizations indicates the region subject to edge effects, the size of which is dependent on the wavelength. This also begs the question, for the maximum wavelengths investigated (~600 microns), what proportion of the input image is actually useable?

We have changed the figure text accordingly to mention the area of edge effects.

Regarding the proportion of the input image that is actually usable at the maximum wavelength, it is 30% of the original image's area. This is stated in the text of section A6.

Experimental evidence that viscous shear zones generate periodic pore sheets that focus mass transport

James Gilgannon¹, Marius Waldvogel¹, Thomas Poulet², Florian Fousseis³, Alfons Berger¹, Auke Barnhoorn⁴, and Marco Herwegh¹

¹Institute of Geological Sciences, University of Bern, 3012 Bern, Switzerland

²CSIRO Mineral Resources, Kensington, WA 6151, Australia

³School of Geosciences, The University of Edinburgh, Edinburgh EH9 3JW, UK

⁴Department of Geoscience and Engineering, Delft University of Technology, Delft, The Netherlands

Correspondence: James Gilgannon (james.gilgannon@geo.unibe.ch)

Abstract.

In experiments designed to understand deep shear zones, we show that periodic porous sheets emerge spontaneously during viscous creep ~~-, forming a hydro-mechanical anisotropy that influences and that they facilitate~~ mass transfer. These findings challenge ~~the current paradigm of~~ conventional expectations of how viscosity in solid rocks ~~-In particular, they show how~~
5 ~~shear zones may actively focus mass transport and highlight the possibility that viscous rocks could locally transition from flow to fracture. Our work demonstrates that viscosity in solids is not directly comparable to viscosity in fluids and this is~~ operates and provide quantitative data in favour of an alternative paradigm, that of the dynamic granular fluid pump model. On this basis, we argue that our results warrant a reappraisal of the community's perception of how viscous deformation in rocks proceeds with time and suggest that the general model for deep shear zones should be updated to include creep cavitation. Through
10 our discussion we highlight how the integration of creep cavitation, and its Generalised Thermodynamic paradigm, would be consequential for a range of important solid Earth topics that involve viscosity in Earth materials, like slow earthquakes, the flow of glacial ice and the tectonics of exoplanets.

1 Introduction

Our existing models for mantle convection, the advance of glaciers and even the dynamics of the seismic cycle all include, and
15 rely on, the concept that solids can be viscous and flow with time. In this sense, the fluid mechanical concept of viscosity is a cornerstone of Geoscience and our view of a dynamic Earth is built around it. In rocks, a record of this viscosity is found in mylonitic shear zones, the largest of which are the deep boundaries of tectonic plates that can reach into the asthenospheric upper mantle (Vauchez et al., 2012). Consequentially, mylonites represent important interfaces in the lithosphere that crosscut different geochemical, geophysical and hydrological domains. This role places them at the centre of discussions on slow earthquakes
20 and the hydrochemical exchange of deep and shallow reservoirs (e.g. Beach, 1976; Fousseis et al., 2009; Bürgmann, 2018). In this context, it is critical to have a robust and complete model of deep shear zones and the viscous rocks in them.

The accepted conceptual model for lithospheric shear zones supposes that there is a mechanical stratification with depth from an upper frictional to lower viscous domain (Sibson, 1977; Schmid and Handy, 1991; Handy et al., 2007). In this model, viscous ~~deformation-creep~~ is a continuous slow background deformation and, at certain conditions, is punctuated by fracturing. It is this ~~episodic fracturing, driven by non-isochoric chemical reactions or frictional embrittlement fracturing, which can have physical (e.g. Beall et al., 2019) or chemical (e.g. Alevizos et al., 2014) driving forces,~~ that creates seismicity and mass transport pathways through the deep Earth (Sibson, 1994). Two core assumptions of this conceptual model are that ~~viscous-creep creep in polycrystalline aggregates~~ mainly contributes to distorting the ~~rock mass (Koeks et al., 1975)-deforming mass (e.g. Poirier, 1985; Hobbs and Ord, 2015)~~ and the large confining pressures of the viscous domain reduce porosity and permeability with compaction (Edmond and Paterson, 1972; Xiao et al., 2006). In contrast, there is a newer paradigm which argues that viscous creep in mylonitic rocks can intrinsically produce a dynamic permeability, called creep cavitation (Fusseis et al., 2009). ~~The presence of such a permeability would fundamentally change the role of viscous rocks during lithospheric~~ (Dimanov et al., 2007; Fusseis et al., 2009). The most well known formulation of this paradigm is the Generalised Thermodynamic model known as the dynamic granular fluid pump (Fusseis et al., 2009). While much of this paradigm remains to be tested, the notion that mylonites generate self sustaining and dynamic pathways for mass transport is radical and consequential for the interpretation of how deep shear zones behave during deformation.

The ~~proposed~~ dynamic permeability is proposed to be created and sustained by-through the opening and closure of syn-kinematic pores, called creep cavities, ~~during creep. In~~ by viscous grain boundary sliding during creep (e.g. Herwegh and Jenni, 2001; Dimanov et al., 2007; Verberne et al., 2017; Chen et al., 2020). In recent years the paradigm has gained traction with many more contributions interpreting the presence of, or appealing to creep cavities in natural samples (e.g. Gilgannon et al., 2017; Précigout et al., 2017; Lopez-Sanchez and Llana-Fúnez, 2018; Giuntoli et al., 2019; Verberne et al., 2020). With the most notable claims involving creep cavities being that in polymineralic viscous shear zones, the formation of creep cavities is postulated to establish their formation establishes an advective mass transport pump (Fusseis et al., 2009; Menegon et al., 2015; Précigout et al., 2019), ~~aid melt migration (Závada et al., 2007)-it aids melt migration (Závada et al., 2007; Spiess et al., 2012)~~ and has even been speculated to nucleate earthquakes (Shigematsu et al., 2004; Dimanov et al., 2007; Rybacki et al., 2008; Verberne et al., 2017; Chen et al., 2020). ~~Currently~~ (Shigematsu et al., 2004; Dimanov et al., 2007; Rybacki et al., 2008; Verberne et al., 2017; Chen et al., 2020). However, much of the ~~evidence supporting this new paradigm-most convincing supporting evidence currently available~~ is limited to deformation experiments on fabricated geo-materials and is generally restricted to grain-scale observations. Hence it has been difficult to evaluate if this phenomenon is extensive and relevant ~~in-natural-at the material scale for natural samples and, moreover, if it is applicable to natural deformations in deep~~ shear zones.

In this contribution we provide unambiguous experimental evidence in a natural starting material that supports, and extends, the paradigm concerning the role of creep cavities in shear zones. We present quantitative results showing that creep cavities are a spatially significant feature of viscous deformation, ~~being generated in periodic sheets throughout the samples. Our analyses are intentionally made over large areas of the experimentally deformed samples in order to contextualise and understand the role of creep cavities at a scale more comparable to those where macroscopic material descriptions are unusually made.~~ We

argue that our results warrant a reappraisal of ~~viscous creep~~ the community's perception of how viscous deformation proceeds with time in rocks and suggest that the general model for viscous shear zones should be updated to include creep cavitation ~~into~~
60 ~~the general viscous shear zone model~~. A key consequence of this would be that the energetics of the deforming system become the keystone of our perspective rather than the mechanics.

2 New results from classical experiments

To make this argument, we have revisited the microstructures of a set of classical shear zone formation experiments ~~performed~~
performed on Carrara marble (Barnhoorn et al., 2004). The torsion experiments were run at a high homologous temperature
65 (T = 1000 K, $T_h = 0.6$) with confining pressure (P = 300 MPa) at constant twist rates. Samples were deformed to large shear strains and recorded the dynamic transformation of undeformed, homogeneous, coarse-grained marbles into fine-grained ultramylonites. The experiments demonstrated that microstructural change by dynamic recrystallisation was concurrent with mechanical weakening and the development of a strong crystallographic preferred orientation. More recently, it was shown that these experiments contain creep cavities and that the pores emerged with, and because of, grain-size reduction by sub-grain
70 rotation recrystallisation (Gilgannon et al., 2020). In this contribution we expand on these observations and present new results that quantify and contextualise the development of porosity inside of an evolving viscous shear zone.

Please refer to the appendix for details of the methods used in the following results.

2.1 Porosity evolution with mylonitisation

75 At very low shear strains, and before any dynamic recrystallisation, pores decorate grain boundaries and appear as trails through large grains ($d \approx \approx 200 \mu\text{m}$, fig. 1a). These pores are likely fluid inclusions trapped in and around the original grains (Covey-crump, 1997) (the ~~porosity-pore~~ density map in fig. 1b reflects this by highlighting the outlines of the initial grain-size). In the experiment run to a shear strain of 5, which is in the midst of significant microstructural adjustment, the porosity has a clearly different character. The pores appear at the triple junctions of small recrystallised grains ($d \approx \approx 10 \mu\text{m}$) and in some ~~case~~
80 ~~cases~~ are filled with new precipitates (fig. 1c). The ~~porosity-pore~~ density map of this experiment highlights that pores appear in clusters that repeat across a large area and are systematically oriented (fig. 1d). Once the microstructure is fully recrystallised ($\gamma = 10.6$), and has reached a microstructural steady state, the porosity forms elongated sheets ~~which also contain new precipitates of phengite and pyrite~~ (fig. 1e). The density map of this experiment reveals that this porosity has become more spatially extensive and also shows a systematic orientation (fig. 1f). ~~The implication of newly precipitated minerals is These~~
85 ~~pore sheets contain new precipitates of mica, Mg-calcite and pyrite, implying~~ that the sheets are permeable and act as mass transfer pathways ~~-(fig. 2). When quantified, it appears that the porosity values before and after dynamic recrystallisation are similar but as strain increases the porosity increases by an order of magnitude (table 1).~~

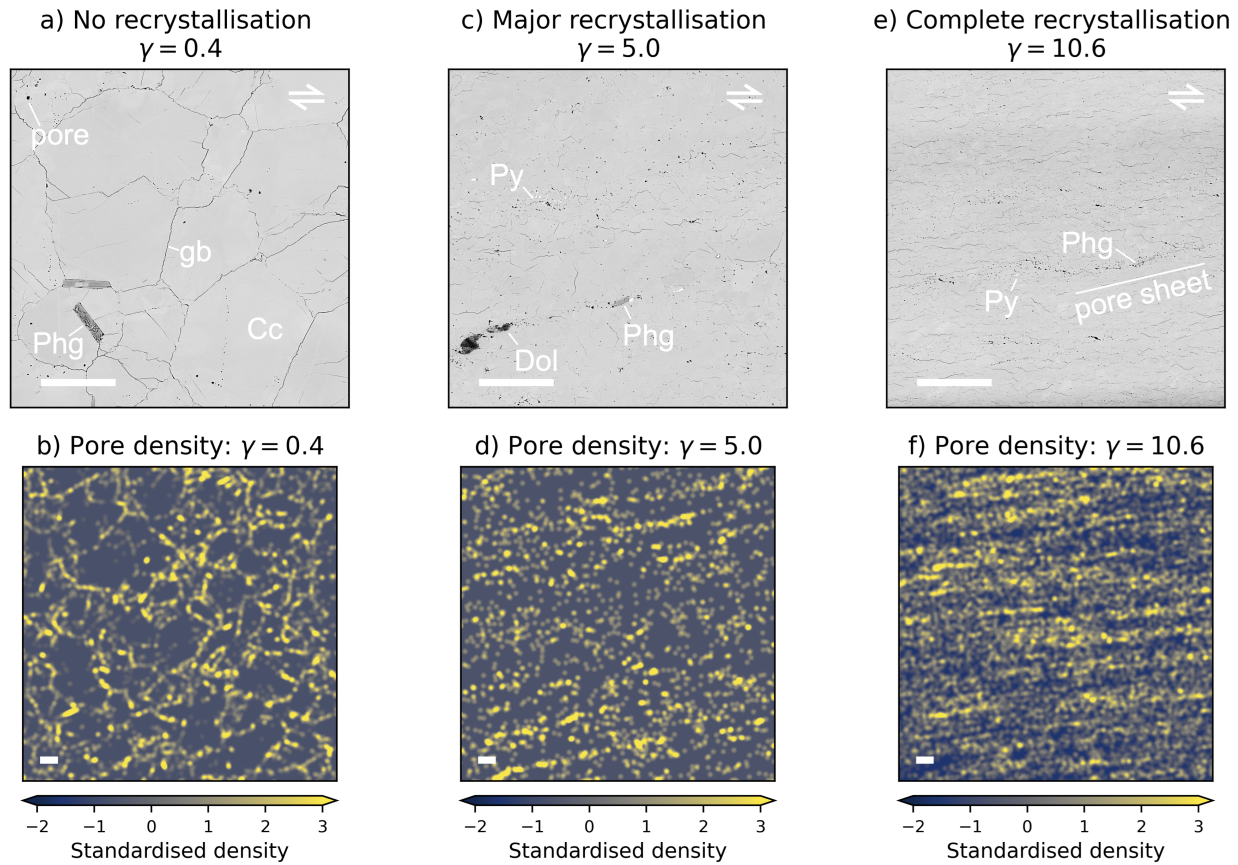


Figure 1. Microstructure and porosity-pore density in samples with increasing strain. The samples document the production of a mylonite through dynamic recrystallisation. Panels a,c and e are backscatter electron images while b, d and f are pore density maps. In all images the white scale bar is 100 μm . The pointed ends of the colour bars refer to the fact that some data values are larger than the max and min of the colour map. (Py = pyrite, Dol = dolomite, Phg = phengite, Cc = calcite, gb = grain boundary).

Table 1. Sample porosity

<u>Sample</u>	<u>γ_{max}</u>	<u>Porosity (%)</u>
<u>PO344</u>	<u>0.4</u>	<u>0.29</u>
<u>PO422</u>	<u>5.0</u>	<u>0.20</u>
<u>PO265</u>	<u>10.6</u>	<u>1.15</u>

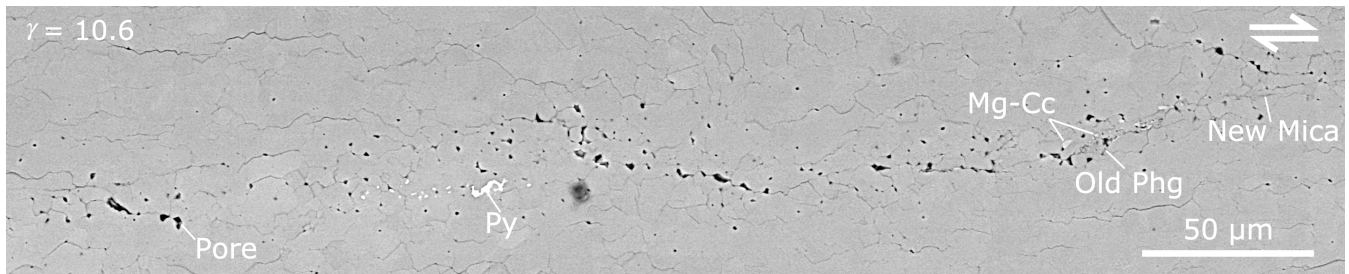


Figure 2. [A more detailed view of the pore sheet labelled in figure 1e. Please find supporting spectra from Energy Dispersive Spectroscopy \(EDS\) in the appendix for the small precipitates. \(Py = pyrite, Phg = phengite, Mg-Cc = magnesium calcite\).](#)

2.2 2D continuous wavelet analysis of pore sheets

We quantify the spatial extent and character of these permeable pore sheets with 2D continuous wavelet analysis. In particular, we use the fully-anisotropic 2D Morlet wavelet (Neupauer and Powell, 2005) to identify features in the pore density maps and expand a 1D scheme of feature significance testing used in climate sciences (Torrence and Compo, 1998) to 2D to filter for noise in the data. Furthermore, by implementing a 2D (pseudo) cone of influence we exclude boundary effects of the analysis at large wavelengths. For details of the wavelet analysis see the Methods section. Fundamentally, wavelet analysis can be thought of as a filter that highlights where the analysed data interacts with the wavelet most strongly. By varying the size and orientation (λ and θ in fig. [2a](#), [3a](#)) of the Morlet wavelet one can isolate significant features in the data and gain quantitative information about them, including orientation, dimension and any spatial frequency.

Wavelet analysis reveals that, in both the partly and fully recrystallised samples, porosity is highly ordered with a strong periodicity and anisotropy. Both samples show two dominant modes of porosity distribution (fig. [2b-3b](#) and c). While the sample is only partly recrystallised, porosity is preferentially oriented at 17 and 15 degrees (measured antithetically in relation to the shear plane, see fig. [2a3a](#)) with wavelengths of ~~245 and 438~~ [~ 240 and ~ 440](#) μm respectively (fig. [2b-3b](#) and fig. [3a4a](#), b and c). This is both contrasted and complemented by the modes found in the fully recrystallised experiment, where the anisotropy is oriented at 9 and 14 degrees with wavelengths of ~~143 and 387~~ [~ 140 and ~ 390](#) μm , respectively (fig. [2e-3c](#) and fig. [3d4d](#), e and f). Interestingly the longer wavelength porosity features in both samples share similar orientations and spacing ($\Delta 1^\circ$, $\Delta 50 \mu\text{m}$). As wavelet analysis does not require features to be periodic to be identified, the periodicity is a result and not an artefact of the analysis. ~~Figure 3g showcases, in more detail, an example of the pore sheets identified by the wavelet analysis.~~

3 Discussion

These results provide an unambiguous foundation for discussing the community's ~~model of viscosity in solids at high homologous temperatures.~~ [Chiefly, its perception of how viscous deformation proceeds with time and more generally the role of viscous](#)

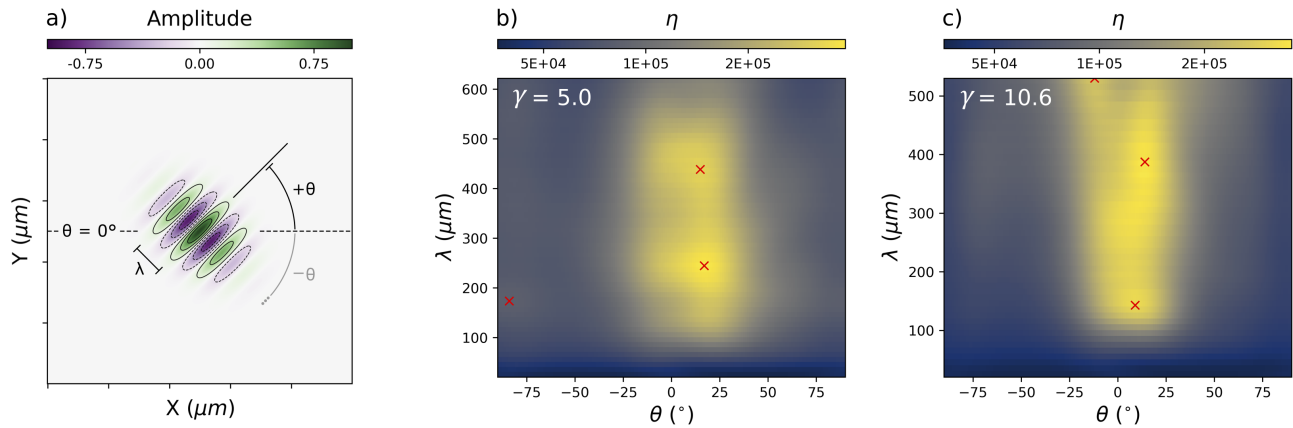


Figure 3. Wavelet analysis of partly ($\gamma = 5.0$) and fully ($\gamma = 10.6$) recrystallised samples. Fig 2a-3a show's a generic 2D Morlet wavelet. The wavelet analysis is conducted by considering the wavelet's interaction with the porosity density maps at each spatial position. This is repeated for different orientations (θ) and wavelengths (λ). Figures 2b and c visualises the wavelet analysis results for the two samples. Peaks in η represent the largest interaction with the wavelet (see section A7 for details). Peaks are identified by local extremes in η and marked with red crosses. We note that two local extremes are not discussed in the text. This is because one was very close to the sensible limit of the analysis ($\theta = -12^\circ$, $\lambda = 530 \mu\text{m}$) defined in appendix section A6 and the other did not correlate with any microstructural features ($\theta = -84^\circ$, $\lambda = 173 \mu\text{m}$).

115 deformation in the conceptual shear zone model. We claim this because our results show that viscous shear zones a mylonitic shear zone deforming viscously can spontaneously develop highly anisotropic periodic porous sheets. Currently, this is not accounted for in our conceptual models and should be integrated as it has important consequences for deformation in nature and periodic porous domains. This is not something that is expected within the prevailing paradigm for the deformation of rocks at high temperatures and pressures. For this reason it is important for us to reconsider the role of mylonites during geochemical, geophysical and hydrological processes in the lithosphere.

3.1 How mylonites could focus mass transport

120 Firstly, we suggest that the presence of periodic, porous sheets in natural shear zones would act to focus fluid during active deformation. Geochemical studies have proposed that the enrichment or depletion of elements in purely viscous shear zones must reflect syn-deformational fluid migration (e.g. Carter and Dworkin, 1990; Selverstone et al., 1991). Our results provide an experimental insight into the microstructure aspects of the syn-kinematic pore network that likely facilitates this fluid transport. Furthermore, this validates the in natural mylonites. The fluid phase in our experiments is not constrained but likely some mix of CO₂, H₂O and Ar that is both inherited from fluid inclusions of unknown compositions in the starting material, from decarbonation of the dolomite present (cf. Delle Piane et al., 2008), the breakdown of some, but not
 125 all, phengite minerals (cf. Mariani et al., 2006) and Ar that has likely diffused into the sample from the confining medium.

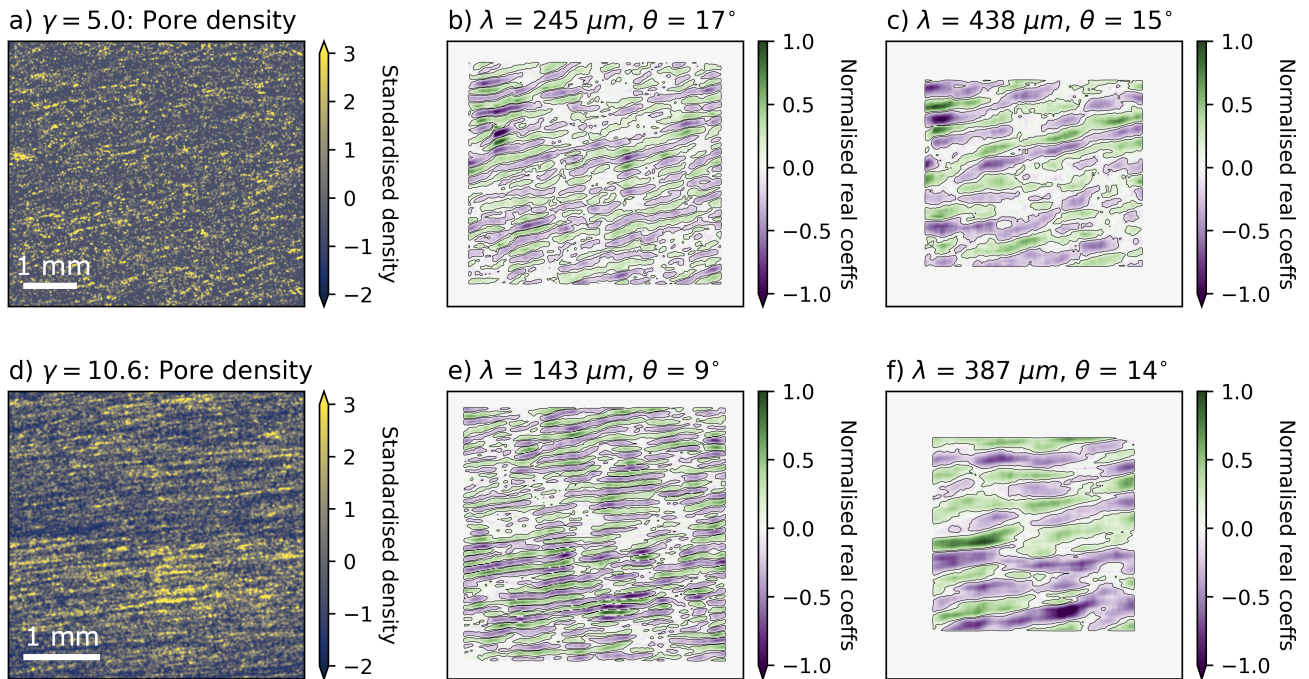


Figure 4. Visualisation of ~~where the~~ results of the wavelet analysis identified convolution with the pore density maps. The anisotropy identified by the dominant peaks in fig. 3 are shown for the partly (figs 3a-e, 4a-c) and fully (figs 3d-f, 4d-f) recrystallised samples. For ~~both samples the visualisation shows the wavelengths each convolution at each wavelength analysed areas are defined for where edge effects may occur and orientations identified by peaks data here is removed, this results in figure 2.~~ Figure 3g presents a more detailed view of the pore sheet-labelled white areas in figure 1 at the edge of figs. 4b-c and e-f (Phg = phengite see section A6 for details). As before, the pointed ends of the colour bars refer to the fact that some data values are larger than the max and min of the colour map.

While it is unclear what the exact composition of the fluid was, the presence of many newly precipitated minerals in pores, and across pore clusters, is evidence that mass was mobile in porous domains during the deformation. Additionally, our results validate the prediction of pore sheets in the dynamic granular fluid pump model (Fusseis et al., 2009) and ~~extends extend~~ it to show that pore sheets can develop spontaneously in homogenous rocks, with a periodic and oriented character. Curiously, our results also seem to suggest that porous domains develop within zones of stable orientation and, possibly, wavelength (approx. 15° from the shear zone boundary with a wavelength of 400 μm). This is consequential because it implies that the emergence of porous sheets is determined by ~~bulk-material-properties some bulk material characteristic (for example, like the elastic moduli)~~ and not by ~~any initial heterogeneity in the material. A question that naturally arises from this is, how would the positions of any initial heterogeneities hosted within the starting material (akin to grain-size variations).~~ What exactly governs the appearance and location of these apparently stably oriented and spaced microstructural adjustments is a clear candidate for important future research as it hints at a challenge to the widely cited role of material inhomogeneity

in determining the location of deformationally induced transformations and fluid pathways often cited in geological studies (e.g. Goncalves et al., 2016; Fossen and Cavalcante, 2017; Giuntoli et al., 2020).

3.2 Does a porous anisotropy affect the mechanics of a mylonite?

140 Two questions naturally arise from our results: (1) how could the presence of periodic porous sheets affect the mechanical
behaviour of mylonites in the deep lithosphere?; and (2) why did the emergence of a spatially extensive and anisotropic
porosity not affected the viscous mechanical state recorded in the original experiments of Barnhoorn et al. (2004)? Answering
these questions is not trivial but there is some ground to be gained by considering the broader Generalised Thermodynamic
literature behind the paradigm of concerning creep cavities and contrasting our results to other experiments where creep cavities
145 have been observed to have an mechanical impact.

3.3 A spontaneous change from flow to fracture

~~We argue that~~

3.2.1 What effect are creep cavities expected to have in a Generalised Thermodynamic model?

In the dynamic granular fluid pump model, creep cavities are predicted to emerge as one of several dissipative processes that act
150 to bring the reacting and deforming rock mass into a thermodynamic stationary state (Fusseis et al., 2009). That is to say that
~~the chief concern of the appearance of pore sheets during deformation could allow for the mechanical behaviour of a viscous~~
~~shear zone to spontaneously change from flow to fracture. This change can never be predicted by flow laws commonly used~~
~~to model viscous deformation in the lithosphere and , if correct, our interpretation challenges the sole use of such flow laws in~~
~~these applications. Two earlier examples of this problem were documented in large strain deformation experiments on synthetic~~
155 ~~gabbros~~ model is that of the energetics of the system with a focus on the rate of entropy production. Theoretically this means
no process is a priori excluded from activating and the most efficient combination of processes that use and store energy act in
congress to produce a thermodynamic stationary state (Fusseis et al., 2009; Regenauer-Lieb et al., 2009, 2015); the system is
neither accelerating or decelerating in a dissipative sense but is in some kind of steady state. In this model, many factors play
a role in determining whether or not creep cavities will affect the mechanical state of the deforming body.

160

One of these factors that may be pertinent to our experiments is the boundary conditions for deformation. It is known from
various types of modelling that different boundary conditions, i.e. constant force vs constant velocity, can promote or inhibit
material instability and localisation (e.g. Fressengeas and Molinari, 1987; Cherukuri and Shawki, 1995; Paterson, 2007). In the
case of constant velocity boundary conditions, like those applied in our torsion experiments, localisation is not expected to
165 occur (e.g. Fressengeas and Molinari, 1987; Paterson, 2007). Indeed, from a Generalised Thermodynamic perspective, when
the boundary conditions are set to a constant thermodynamic flux, i.e. a constant velocity (like the experiments we revisit),
the dissipative conditions are fixed and the material is forced to meet them through the activation of as many dissipative

micro-mechanisms, at as many positions in the rock, as necessary (cf. Veveakis and Regenauer-Lieb, 2015; Guével et al., 2019). Conducting a deformation experiment in this fashion means that the onset of a localising instability can be missed because the rock is not allowed to incrementally adjust to an incrementally applied energy input (e.g. Peters et al., 2016). This does not prohibit the possibility of local microstructural differences developing but it does mean that, at the scale of the material a distributed deformation can remain favourable despite a heterogeneous microstructure. This observation of a stable but heterogeneous microstructure suggests that the size of the heterogeneities produced are not sufficiently large to impose further localisation. In the work of Shawki (1994) it was shown that thermal perturbations below a critical wavelength would not impose localisation during constant velocity boundary conditions. If the variation in creep cavity domains reflect different amounts of work being dissipated locally, and hence heat being produced, then one can see that the shorter wavelength porous domains, which reflects the size of actual pore sheets (fig. 2), are below the size of the thermal heterogeneities that were found to impose localisation in the constant velocity models (see fig. 5 in Shawki, 1994). Thus, from a Generalised Thermodynamic perspective, the boundary conditions of our experiments may, in part, explain why we do not see an obvious mechanical effect of the porosity with ongoing straining: once the steady state microstructure is attained, the sample is in a thermodynamic stationary state for the imposed boundary velocity that favours a distributed deformation.

A constant force boundary condition is predicted to produce instability and localisation in rock deformation at high homologous temperatures (e.g. Fressengeas and Molinari, 1987; Paterson, 2007). It is often assumed that plate boundaries in nature will be under such a boundary condition (cf. Alevizos et al., 2014) and in this instance the presence of anisotropic domains of porosity may have a different impact than in our experiments. For example in experiments, not dissimilar in geometry to our own, run on olivine, it was found that localisation did indeed occur at constant force conditions and not for constant velocity (Hansen et al., 2012). At a constant force this localisation was expressed both in the microstructural adjustments (with the development of an oriented foliation and domains of varying grain-size) and in the mechanical behaviour of the olivine aggregates (noted by a continual weakening of the samples beyond a shear strain of 0.5). If we for a moment speculate on how our experiments may have proceeded under constant force boundary conditions it could be that porous domains emerge with some similar modes of periodicity to those observed under a constant velocity but in this case they might provide the sites for some kind of instability. For example, in our hypothetical case, pore sheets may aid in establishing features like the high frequency foliation and lower frequency domains of grain-size variation observed by Hansen et al. (2012) (e.g. figs. 5c and d and fig. 9a in Hansen et al. (2012)). Of course our speculation is only that and this line of argument requires new experimental testing that is beyond the scope of our revisiting of the classical experiments of Barnhoorn et al. (2004). What it does highlight is that viscous deformation in mylonites requires more research to understand exactly when and where a periodic occurrence of creep cavities could have a mechanical impact.

3.2.2 A comparison to other experiments that developed domains of creep cavities

In this context, there are four other experimental works in which creep cavities were documented to develop that are worth comparing to our results. All of these experiments were run in torsion at high confining pressures and homologous temperatures

on synthetic dolomite (Delle Piane et al., 2008), synthetic gabbro (Dimanov et al., 2007) and synthetic anorthite aggregates (Dimanov et al., 2007; Rybacki et al., 2008). In those experiments, creep fractures were shown to evolve out of deformation characterised by strain invariant mechanical parameters for (Rybacki et al., 2008, 2010). All experiments developed creep cavities in oriented and spaced domains during linear viscous flow. In the gabbroic and some of the anorthitic samples, these porous domains became sites for the generation of instabilities known as creep fractures (Dimanov et al., 2007; Rybacki et al., 2008, 2010). When one compares the four experimental sets to our samples and one another, it is clear there are many differences and similarities. Firstly, the starting materials are all compositionally different and have various initial mean grain sizes, grain shapes and grain size distributions. Secondly, all four of these experiments use fabricated samples in comparison to our natural Carrara marble samples. Thirdly, when domains of creep cavities did emerge in the four experiments, some produced bands that were broadly a mirrored orientation to our results around the shear plane (see fig. 14 and 16 in Dimanov et al. (2007); fig. 1 in Rybacki et al. (2008); fig. 6 in Rybacki et al. (2010); and fig. 2 in Spiess et al. (2012)) with others being similarly oriented to our results (see fig. 8a in Delle Piane et al. (2008) and fig. 5 in Rybacki et al. (2010)). Lastly, for the gabbroic and anorthitic experiments these oppositely oriented porous domains were reported to evolved into fractures while those domains of a similar orientation to our results did so less or not at all (Dimanov et al., 2007; Rybacki et al., 2008, 2010), and never in the dolomite experiments where linear viscous flow. Our experiments were also found to have constant mechanical parameters with strain (Barnhoorn et al., 2004) was maintained (Delle Piane et al., 2008). It is not clear what critical condition leads some to fracture and others to not: for example, is it the local pore density or the widths of the porous domains that controls if a fracture develops? While it is hard to draw any categorical conclusions from the comparison of these experiments, it is noteworthy that in each experimental case the mechanical data recorded a viscous deformation, regardless of whether a fracture instabilities occurred or not. This point draws attention to a conclusion already made in the seminal work of Dimanov et al. (2007), “[c]learly, the ‘microstructural state’ is not obviously representative of the ‘mechanical state’...”. If this holds true for mylonites in nature then it opens an ambiguity over how the deformation of a mylonite will proceed with time: will it fracture, or will it flow?

3.2.3 Is a flow law enough to describe a mylonite?

Our results, and those of the four other experiments described above, suggest that mylonites of various compositions develop complicated microstructures that for an unknown set of critical conditions can facilitate a spontaneous mechanical change from flow to fracture. While there are many ways to incorporate history-dependence into flow laws that account for some microstructural change (cf. Renner and Evans, 2002; Barnhoorn et al., 2004; Evans, 2005) it does not seem that this kind of rate equation would capture the differences between ours and the four other experiments described. For example, a flow law that integrated strain (e.g. Hansen et al., 2012) would not be able to account for why some of the five experiments fractured at shear strains below 5 (e.g. Dimanov et al., 2007; Rybacki et al., 2008, 2010) with others flowing up to a shear strain of 50 with no fractures developing (Barnhoorn et al., 2004). We suggest that this potential disconnection between the microstructure and mechanics of a mylonite makes it impossible to use only one rate equation to describe how a shear zone may deform with time.

235

This point complements the fact that the dynamic granular fluid pump model (Fusseis et al., 2009), which our work tests aspects of, requires the consideration of energy, mass and momentum balance alongside rate equations for irreversible physical deformation (like plastic or viscous flow laws) and both reversible and irreversible chemical processes (Fusseis et al., 2009; Regenauer-Lieb et al., 2015). These different dissipative processes act at different diffusive length scales and are predicted to account for the geometry and temporal variation of several phenomena that all act synchronously during a deformation (cf. Regenauer-Lieb et al., 2015). In this perspective a flow law(s) is necessary but not sufficient to fully describe a deformation, with the balancing of the energy equation being of chief importance. Said another way, many thermally activated rate equations for physical processes may compete to dissipate energy and collectively produce a bulk mechanical diffusivity (Veveakis and Regenauer-Lieb, 2015). While our results cannot speak to all of these claims, they do show that there is some validity to the predictions of this newer paradigm, namely the emergence of pore sheets. This generally adds weight to older discussions about the possible need for a more complex view of deformation in mylonites (Evans, 2005; Dimanov et al., 2007) and suggests further testing is needed of the Generalised Thermodynamic ideas behind the paradigm concerning creep cavities.

3.3 Some consequences of incorporating creep cavities into the conceptual shear zone model

There are several enigmatic observations that are not well accounted for in the current conceptual model for lithospheric shear zones. To name a few: there is field evidence of frictional melting in the deep crust (Hobbs et al., 1986); the intrusion of dykes during upper amphibolite facies conditions (Weinberg and Regenauer-Lieb, 2010) and the fact that some geophysical data suggest that slow earthquake phenomena can occur at depths below the seismogenic zone (Wang and Tréhu, 2016). If the new evidence that we present, that mylonites can develop periodic porous domains during a viscous deformation, is incorporated into our conceptual model for lithospheric shear zones many new possible explanations emerge for otherwise hard to explain observations.

In the case of dyke intrusion at high grade conditions, the work of Weinberg and Regenauer-Lieb (2010) in fact already invoked creep cavities and their coalescence into creep fractures as the responsible mechanism for allowing dyking to occur. While our results do not show the development of creep fractures, they forward the speculative argument of Weinberg and Regenauer-Lieb (2010) that creep cavities will occur during ductile shearing in rocks. Additionally, recent experiments on calcite gouges made observations of creep cavities and argued that their formation allowed the gouge to transition from flow to friction (Chen et al., 2020). While these were lower temperature experiments than our own, they reinforce the notion that rocks could spontaneously transition from a viscous rheology to another mechanical state. This is relevant for observations of deep seated frictional melting where the presence of a porous anisotropy in mylonites may facilitate changes to some kind of granular or frictional mechanical state that is otherwise unexpected. Also in the case of quartz and calcite-dominated crustal-scale shear zones there often exists a peculiar relationship between viscous strain localization in ultramylonites, fracturing and precipitation of synkinematic veins/fluid flux within these ultramylonites (e.g. Badertscher and Burkhard, 2000; Herwegh and Kunze, 2002; Herwegh et al., 2005; Haertel et al., 2005). In the wake of our results, it is tempting to propose that this syn-kinematic veining may be related to an interplay of fluid transport and we speculate that the pore sheets we observe could evolve into creep fractures in a natural setting. We suggest

270 ~~this because natural conditions are more varied, both in magnitude and in time, than those tested by our experiments. In this natural setting a fluid-filled pore sheet may become mechanically unstable and collapse during deformation. This process may even cascade and the instability of one sheet may propagate to others, which may explain the anisotropic porous domains. This is especially so for cases like the deeper portions of the basal shear zones of the nappes of the Helvetic Alps, where veining is observed to broadly increase with proximity to ultramylonitic shear zones (cf. Herwegh and Kunze, 2002) that are expected~~
275 ~~to be purely viscous in our current mechanical paradigm of the crust. Moreover, any instability of pore sheets in natural plate boundaries may factor into explaining~~ how both ambient and teleseismically triggered tremors can occur at depths below the seismogenic zone (Wang and Tréhu, 2016). This ~~interpretation places pore sheets,~~ could place sheets of creep cavities alongside brittle fracturing and non-isochoric chemical reactions ~~,~~ as the potential nuclei of slow earthquake phenomena. ~~Furthermore,~~
280 ~~as~~ As the emergence of creep cavities was linked to dynamic recrystallisation (Gilgannon et al., 2020), a process expected throughout the lithosphere, the ~~hydro-mechanical porous~~ anisotropy presented here would allow slow earthquake phenomena to occur across a range of metamorphic conditions and mineralogical compositions (Peacock, 2009).

4 Conclusions

In summary, the current paradigm of viscosity that is borrowed from fluids is not a completely adequate analogy for solid geomaterials. We ~~have shown that as rocks deform viscously, they spontaneously develop a hydro-mechanical anisotropy. This~~
285 ~~would not be expected within the current paradigm – claim this because we observe that during the formation of a mylonite, that was recorded to possess viscous mechanical properties, a heterogeneous microstructure of periodic porous domains emerged. The current paradigm of viscosity in rocks does not expect this to occur and we have discussed how this observation of pore sheet formation during viscous deformation is seen in at least four other experiments of differing compositions. The porous anisotropy we observe likely has a role to play in both the transport of mass and the mechanics of the lithosphere.~~ On this
290 basis, we advocate for an update to the current concept of viscosity at high temperatures and pressures in rocks to include the ~~viscous hydro-mechanical periodic porous~~ anisotropy we have presented. Our discussion has explored some of the possible consequences of changing our paradigm and moving forward these speculations should be ~~integrated and further~~ tested. As the viscosity of solids is a cornerstone of Geoscience, our results have farther reaching implications than the conceptual shear zone model and may even be relevant for other scenarios where solid state deformation is modelled with viscous rheologies,
295 like glacial flow (e.g. Egholm et al., 2011) and tectonics on ~~exoplanets~~ exoplanets (e.g. Noack and Breuer, 2014).

Code and data availability. Available from James Gilgannon.

Appendix A: Methods

The results of the main manuscript come from the investigation of 3 experimental samples (see table A1). Each sample was imaged using scanning electron microscopy, segmented and analysed. In the following the data acquisition, processing and analysis used will be outlined. For a description of the starting material or the original experimental procedure please refer to Barnhoorn et al. (2004) and Gilgannon et al. (2020).

A1 Acquisition of large backscatter electron mosaics

Three large BSE maps were acquired on a Zeiss Evo 50 SEM with a QBSD semiconductor electron detector (acceleration voltage = 15 kV; beam current \approx 500 pA). In each case the maps were stitched together by the Zeiss software Multiscan. The pixel dimensions and scales are listed in table A2.

Table A1. Experimental samples revisited

Sample	$\dot{\gamma}$	γ_{max}	Amount of recrystallisation
PO344	3×10^{-4}	0.4	None
PO422	3×10^{-4}	5.0	Major ^a
PO265	2×10^{-3}	10.6	Complete ^b

^a 65-90 % as classified by Barnhoorn et al. (2004)

^b 90-100 % as classified by Barnhoorn et al. (2004)

Table A2. Dimensions and resolutions of mosaics

Sample	γ_{max}	Pixel dimensions	Scale (px : μm)
PO344	0.4	15000 x 13944	1 : 0.36
PO422	5.0	8745 x 7392	1 : 0.55
PO265	10.6	21127 x 20494	1 : 0.16

A2 Segmentation for porosity

We used the segmentation, labelling and filtering work flow described in Gilgannon et al. (2020) [for open pore space](#). In this work flow grain boundaries must be filtered for by using each labelled feature's aspect ratio. Specifically, the data is filtered to remove features with aspect ratios greater than 4. Figure S1-A1 shows all features initially labelled as porosity by the segmentation process in each sample. These are plotted for their area and perimeter, while colour coded for aspect ratio. In each data set there are two trends:

1. Features with aspect ratios > 4 that show area-perimeter relationships for lines of widths between 0.25-1.25 μm

2. Features with aspect ratios < 4 that do not show area-perimeter relations of a line

Based on this criteria, only features with aspect ratios of < 4 are considered as pores. The ~~centroids of~~ centres of mass of features meeting this criteria were then extracted and used in the kernel point density analysis.

A3 Kernel density estimator maps

At the first instance, one of the major difficulties in understanding the relationship of micron scale features across millimetres is simply visualising the problem. We utilised the kernel density (KDE) for point features function in ESRI's ArcGIS v10.1 software to overcome this issue. This has the effect of converting point data, that only tell us something about individual pores, to a map that considers the distribution of pores and, in part, their relation in space.

We manually set the output cell size and search radius to $1 \mu m$ and $20 \mu m$, respectively. The kernel smoothing factor was automatically calculated with reference to the population size and the extent of analysis and contoured based on a $1/4 \sigma$ kernel. We specifically did not use the default search radius (calculated with Silverman's Rule of Thumb). Our intention here was to retain as much data as possible in the visualisation. In this way we visualised local neighbourhoods and produced an image for further analysis that had not been overly smoothed. It was these density maps that we then quantitatively analysed with 2D continuous wavelet analysis.

A4 2D Continuous wavelet analysis

Wavelets are highly localised waveforms that can be used to analyse signals with rising and falling intensity. Our images are such signals. Simply put, wavelets can be used to reveal the location (in space or time) and the frequency at which the most significant parts of a signal can be found. Continuous wavelet analysis is the particular wavelet-based method that we employ in this contribution.

To identify features at different frequencies the wavelet is stretched over what are ~~known~~ known as different scales (a). The scales relate to the central frequency of the wavelet, which in turn can be related to the wavelength (λ):

$$\lambda = \frac{4\pi a}{k_0 + \sqrt{k_0^2 + 4}} \quad (A1)$$

where k_0 is the wavenumber.

In the broadest sense, a wavelet can be seen as a filter that finds peaks in an image. To do this it is shifted around the spatial domain (\mathbf{x}) of an image, by way of the shift parameter (\mathbf{b}), and this is repeated at different scales to find peaks. In this way features of different sizes can be located in space and in scale: short wavelengths highlight small features and long wavelengths larger ones. In this contribution, we utilise the fully anisotropic Morlet wavelet (Neupauer and Powell, 2005) because it also

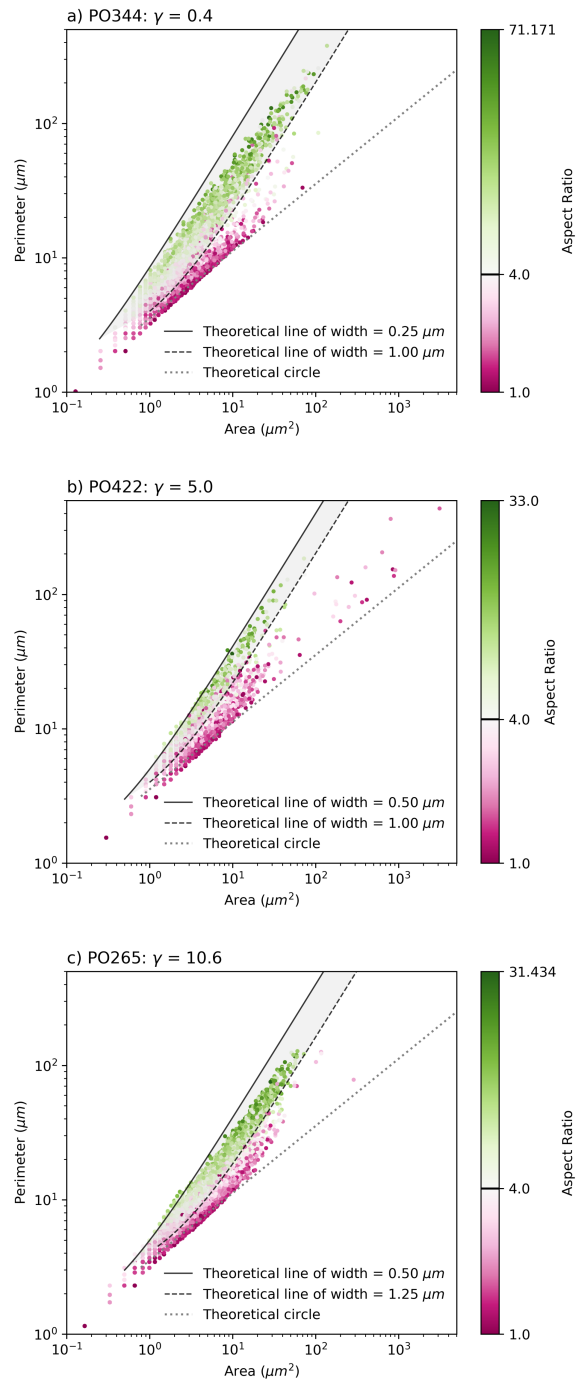


Figure A1. Filtering criteria for grain boundaries and pores.

allows features of varying orientation to be identified. The wavelet is considered to be fully anisotropic because it produces in-phase elongation along the wave vector, such that the wavelet can be rotated and maintain its anisotropy. The wavelet takes the form:

$$\Psi(\mathbf{x}, \theta, L) = e^{i\mathbf{k}_0 \cdot \mathbf{C}\mathbf{x}} e^{-1/2(\mathbf{C}\mathbf{x} \cdot \mathbf{A}^T \mathbf{A} \mathbf{C}\mathbf{x})} \quad (\text{A2})$$

Where θ , L , \mathbf{k}_0 , \mathbf{C} and \mathbf{A} are the angle for the rotation matrix, ratio of anisotropy, wave vector, rotation matrix and anisotropy matrix, respectively. The non-scalar terms are given by:

$$\mathbf{k}_0 = (0, k_0), k_0 > 5.5 \quad (\text{A3})$$

In this study we use $k_0 = 6.0$.

$$\mathbf{C} = \begin{bmatrix} \cos \theta & -\sin \theta \\ \sin \theta & \cos \theta \end{bmatrix} \quad (\text{A4})$$

This rotation matrix rotates the entire wavelet by θ , which is defined as positive in a counter-clockwise direction with respect to the positive x axis (see fig. 2-3 of the main manuscript).

$$\mathbf{A} = \begin{bmatrix} L & 0 \\ 0 & 1 \end{bmatrix} \quad (\text{A5})$$

Where the ratio of anisotropy (L) is defined as the ratio of the length of the wavelet perpendicular to θ over the length parallel to θ . In this way, values of $L < 1$ represent extreme anisotropy parallel to the angle of the wavelet.

We chose to use an anisotropy ratio of $L = 1.5$ (see fig. S2A2). This was done because the input images are kernel density maps and the estimator used is circular. We wanted our wavelet to utilise its inherent anisotropy and angular selectivity to identify extended concentrations of the estimator that would appear as elliptical clusters of circles. We did not use an $L < 1$ as these wavelets anisotropies are too far from the shapes expected from the features we investigated (Torrence and Compo, 1998). If, for example, we had been investigating linear features like fractures we would have used a more anisotropic wavelet shape (for example, $L = 0.5$).

To ensure that the total energy of the analysing wavelet is independent of the scale of analysis the relationship between the wavelet (eq.A2) and the mother wavelet is:

$$\Psi_{a,\mathbf{b}}(\mathbf{x}, \theta, L) = \frac{\sqrt{L}}{a} \Psi\left(\frac{\mathbf{x} - \mathbf{b}}{a}, \theta, L\right) \quad (\text{A6})$$

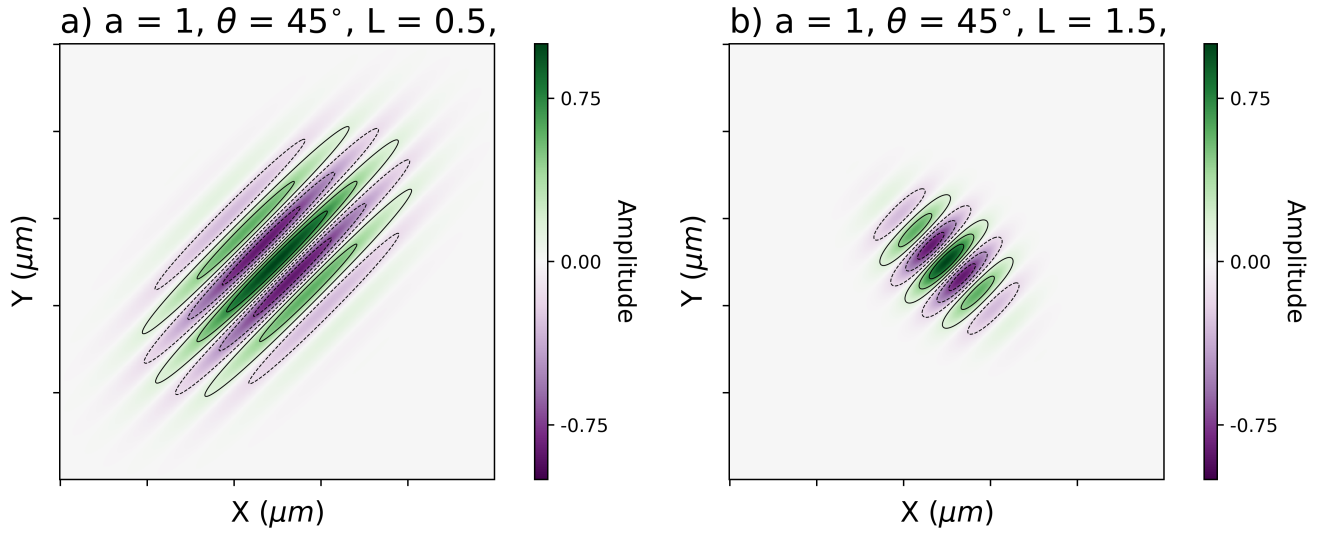


Figure A2. Examples of how a wavelet changes with the anisotropy ratio (L).

To be clear, we refer, above, to energy in the generalized sense of signal processing.

370 Our input images for wavelet analysis are ~~8-bit-32-bit~~ kernel density maps ~~of pore-centroids~~ for the centres of mass of open pores. Each density map can be considered as an intensity function ($\mathbf{I}(\mathbf{x})$) who's magnitude limits are ~~0 and 255~~ that of the KDE density calculation. We standardise each input image such that,

$$\mathbf{I}_{std}(\mathbf{x}) = \frac{\mathbf{I} - \mu}{\sigma} \quad (\text{A7})$$

375 Where μ and σ are the image's mean and standard deviation. This is because the best results of wavelet analysis are achieved on a zero-mean random field (Neupauer and Powell, 2005).

It is on this new standardised image that we preform the wavelet transformation. The wavelet transformation of $\mathbf{I}_{std}(\mathbf{x})$ is a convolution with the analysing wavelet:

$$\mathbf{W}_{\Psi} f(\mathbf{b}, a, \theta, L) = \frac{\sqrt{L}}{a} \int_{-\infty}^{\infty} f(\mathbf{x}) \bar{\Psi} \left(\frac{\mathbf{x} - \mathbf{b}}{a}, \theta, L \right) d\mathbf{x} = \frac{\sqrt{L}}{a} f(\mathbf{b}) * \bar{\Psi} \left(-\frac{\mathbf{b}}{a}, \theta, L \right) \quad (\text{A8})$$

380 Here, $*$ is the convolution and the overbar denotes the complex conjugate. The convolution is evaluated by taking the inverse fast Fourier transform of the products of the Fourier transforms of $f(\mathbf{b})$ and $\bar{\Psi}(-\mathbf{b}/a, \theta, L)$. This wavelet and the convolution follow those outlined in Neupauer and Powell (2005).

A5 Defining significance

385 As outlined above, wavelet analysis will highlight regions of an image where the wavelet and the image interact strongly. This interaction alone is not enough to say that what the wavelet highlighted is relevant when compared to any expected noise in the image. Therefore, it is important to know if the areas highlighted by the wavelet are significant. To define what is significant in the analysis we adopt the method outlined in Torrence and Compo (1998).

The general assumption of the null hypothesis is that the image analysed has some mean power spectrum (P_k , see equation 390 16 in Torrence and Compo (1998)), related to a background geophysical process(es). If the wavelet power spectra is found to be significantly above this background spectrum then the feature is *a real anomaly* and not a result of the assumed background process(es).

To test the null hypotheses, the local wavelet power spectrum at each scale (following equation 18 in Torrence and Compo 395 (1998)) must be considered:

$$\frac{|W_{\mathbf{b}}(a)^2|}{\sigma^2} \implies \frac{1}{2}P_k\chi_2^2 \quad (\text{A9})$$

Where $|W_{\mathbf{b}}(a)^2|$ is the local power, σ^2 is the variance, \implies indicates ‘is distributed as’ and χ_2^2 represents a chi-square distribution with two degrees of freedom. Using the relation in eq. A9 one can find how significantly the local wavelet power deviates from the background spectrum. To do this, the mean background spectrum, P_k (where k is the Fourier frequency), is 400 multiplied by the 95th percentile value of χ_2^2 to give a 95% confidence level. As the local wavelet power is distributed equivalently, this confidence level can be used to contour the global wavelet power ($|W_{\Psi}^2|$). The result allows the identification of data that has a 95% chance of not being a random peak from the background spectrum (see fig. [S3A3](#)).

In this contribution we adopted a white noise model as our background spectra. White noise is a random signal that assumes 405 a uniform power across frequencies. We chose this because we wish to identify when porosity density is non-random and, based on our knowledge of the active processes, we consider that any noise will be uniform across the scales of analysis. We make this assumption about the background spectra for the following reasons.

The experiments we revisit are non-localising at the sample scale and are considered as the exemplar of a sub-solidus, 410 homogenous, viscous deformation. The prevailing assumption for such a sample being deformed is that the microstructural change will first occur where locally favourable conditions allow. For example, some poorly oriented grains may develop more

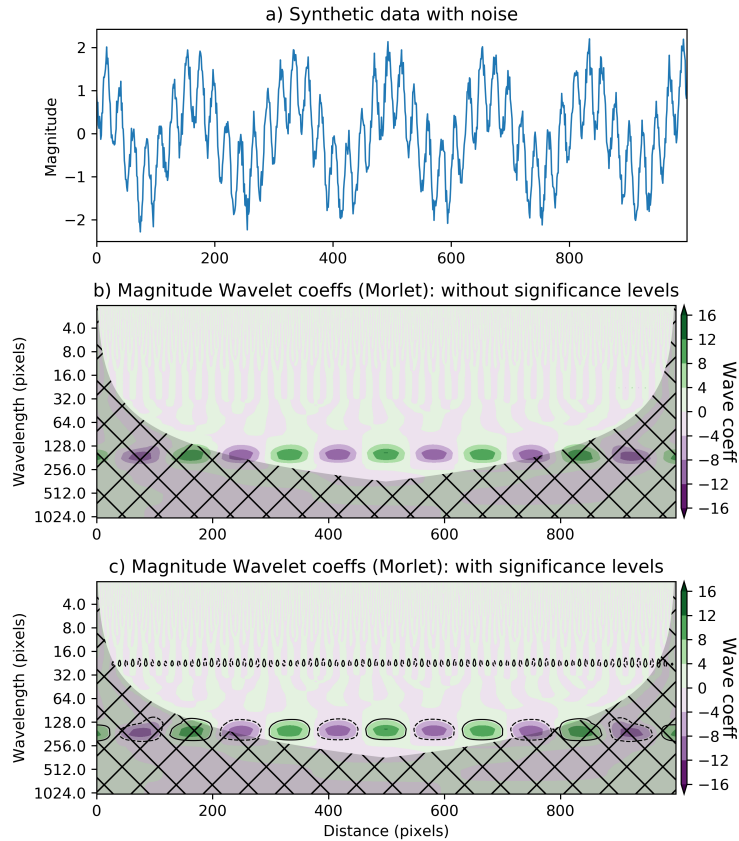


Figure A3. Example of why significance test is needed. a) is a 1D synthetic, noisy, signal made of 2 waves, of different wavelengths. b) and c) present the 1D wavelet transformation of (a) with a 1D Morlet wavelet: in (b) the result is only visualised, while in (c) the significance test is also visualised. In both, the hatched area contains edge effects and is delimited by a 1D cone of influence. The contouring in (c) shows domains that are within the 95% confidence level of not being white noise. The contours highlight values that are both positively and negatively larger than the white noise model. The takeaway message is that the significance test is needed to accurately identify regions of ‘real anomaly’.

deformation induced defects and be prone to recrystallise earlier than other grains. The general distribution of grain orientations is determined by the starting material’s texture, which in the case of Carrara marble is random (Pieri et al., 2001). Therefore, as there is not any initial anisotropy in grain orientations, it is expected that porosity will form randomly in space at favourable sites in the microstructure. Any deviation from this expectation is of interest to us. For these reasons, we use a white noise model as our background spectra and it forms the reference for testing where the porosity density is non-random.

As stated in the main text, it was shown for our experiments that creep cavities emerged with, and because of, grain size reduction by sub-grain rotation recrystallisation (18)(Gilgannon et al., 2020). The white noise null hypothesis used supposes

420 that this grain size change and porosity development occurred with no preference in space or frequency. By using this as our null model we can show when the wavelet analysis produces interactions that are very unlikely to have occurred randomly, and highlights heterogeneity and anisotropy in the porosity density maps.

A6 Defining limits of the analysis

As images have finite length and width the analysing wavelet will misinterpret these edges and produce erroneously positive
425 results. To avoid this one may use padding but ultimately the problem will remain (Torrence and Compo, 1998). Instead, we have chosen to implement a 2D cone of influence (COI). Starting from the edge of the image, the COI defines a zone in which data will likely suffer from edge effects (see area outside of red contour in fig. S4b-A4b). The zone increases proportionally with the wavelet scales. We consider our 2D COI as a pseudo-COI because we simply project two 1D COIs across the 2D surface. We use the e-folding time defined by Torrence and Compo (1998) for their 1D Morlet wavelet, which is $\sqrt{2a}$. For both
430 the y and x axis of the input image we can calculate the appropriate length 1D COI. Each of these 1D COIs is calculated for the set of discrete scales (a) defined for the wavelet transformation. At each scale, the y and x axis COIs are projected to produce a contour that defines the 2D COI at each scale (see fig. S4b-A4b and c).

In this way, our COI does not account for the wavelet's shape and anisotropy. While this means our COI is not the correct
435 mathematical solution for defining where edge effects end for this 2D wavelet, it is a best first attempt at defining a limit to the analysis. We then delete data that lies within the COI. Furthermore, we define a *sensible* limit to the largest relevant scale of analysis by only considering scales which have *edge-effect-free* windows that are greater than 30% of the original image size.

A7 Visualising wavelet results

Figure 2-3 of the main manuscript uses the global measure η (Neupauer et al., 2006) to investigate peaks in the data. Here we
440 define η as:

$$\eta\eta(a, \theta, L) = \int |W_{\Psi} W_{\Psi}^2| d\mathbf{b} \quad (\text{A10})$$

As we use only one value of anisotropy, η can be visualised to reveal information about peaks in orientation and scale. To quantitatively identify peaks in η we use the h_maxima function (where $h = 0.03$) of the Scikit-image python library (van der Walt et al., 2014).

445 A8 Energy Dispersive Spectroscopy (EDS) spectra of small precipitates in pore sheet

Point analysis was used to collect spectra with Energy Dispersive Spectroscopy (EDS) of the small precipitates in the pore sheet presented in figure 2 of the main manuscript. This data is shown alongside a higher resolution BSE image taken under high vacuum on the same Zeiss Evo 50 SEM described above.

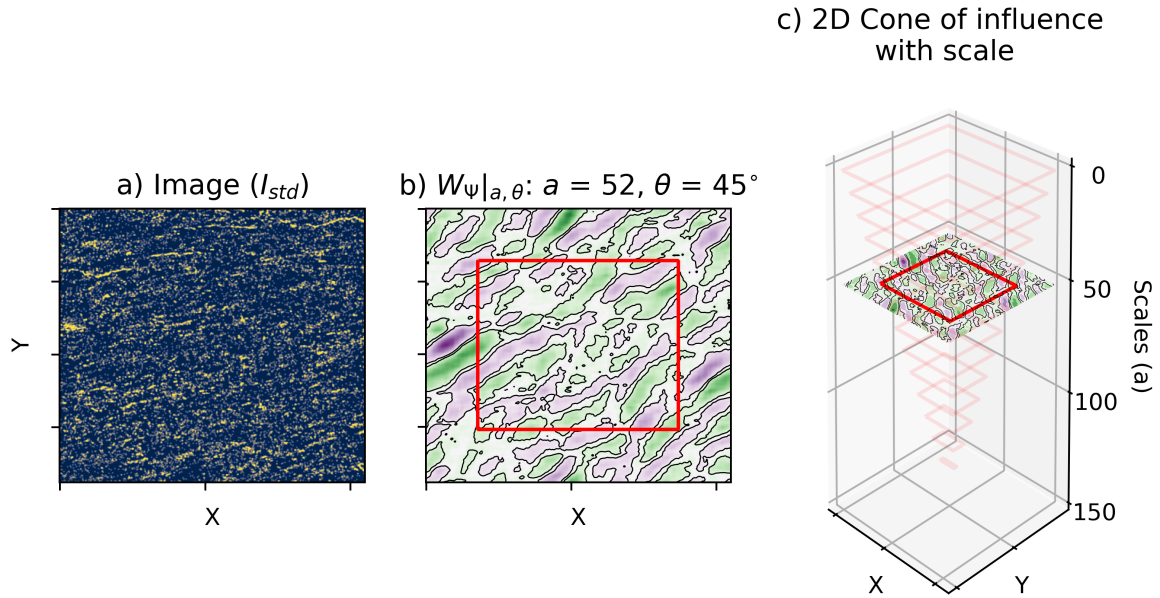


Figure A4. Defining the limits of the analysis across scales. For some image (a), an arbitrary wavelet transformation is visualised at an arbitrary scale and angle (b). Here the black contours enclose data that is within the 95% confidence level. Overlaying this is a red contour which delimits the zone of possible edge effects of the analysis. At this scale this is a slice of the cone of influence (COI). c) visualises the COI across scales. As the scale, and therefore the wavelength of the analysing wavelet, increase, the zone without edge effects decreases. For the purposes of demonstration, data within the COI has not been removed in this figure.

Author contributions. J. Gilgannon, T. Poulet, A. Berger and M. Herwegh designed the study. J. Gilgannon and M. Waldvogel implemented the wavelet method. A. Barnhoorn ran the original experiments. All authors were involved in the interpretation of the results and the writing of the final manuscript.

Competing interests. There are no competing interests.

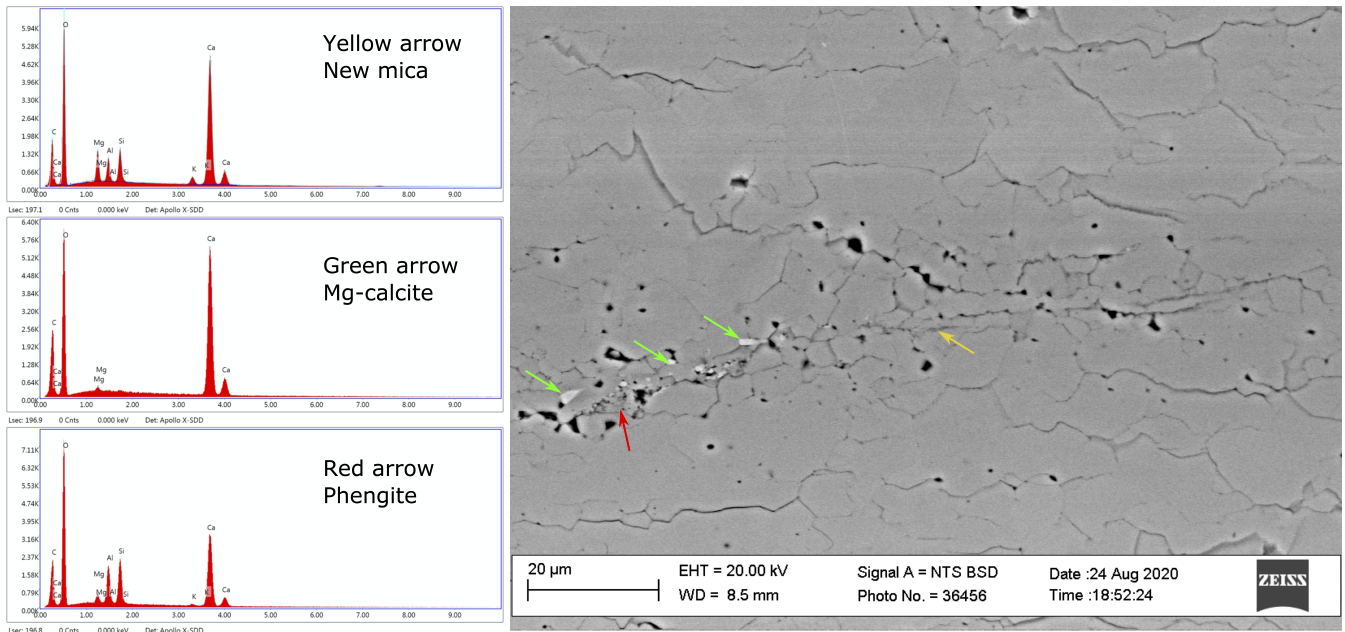


Figure A5. [Energy Dispersive Spectroscopy \(EDS\) spectra of small precipitates in pore sheet shown in figure 2 of the main manuscript.](#)

Acknowledgements. This work was financially supported by the Swiss National Science Foundation (SNSF; grant number 162340). We would also like to thank Klaus Regenauer-Lieb for several stimulating discussions about the role of creep cavities and rock rheology in general.

References

- Alevizos, S., Poulet, T., and Veveakis, E.: Thermo-poro-mechanics of chemically active creeping faults. 1: Theory and steady state considerations, *Journal of Geophysical Research: Solid Earth*, 119, 4558–4582, <https://doi.org/10.1002/2013JB010070>, 2014.
- Badertscher, N. and Burkhard, M.: Brittle–ductile deformation in the Glarus thrust Lochseiten (LK) calc-mylonite, *Terra Nova*, 12, 281–288, <https://doi.org/10.1046/j.1365-3121.2000.00310.x>, 2000.
- 460 Barnhoorn, A., Bystricky, M., Burlini, L., and Kunze, K.: The role of recrystallisation on the deformation behaviour of calcite rocks: large strain torsion experiments on Carrara marble, *Journal of Structural Geology*, 26, 885–903, <https://doi.org/10.1016/j.jsg.2003.11.024>, 2004.
- Beach, A.: The Interrelations of Fluid Transport, Deformation, Geochemistry and Heat Flow in Early Proterozoic Shear Zones in the Lewisian Complex, *Philosophical Transactions of the Royal Society of London. Series A, Mathematical and Physical Sciences*, 280, 569–604, 1976.
- 465 Beall, A., Fagereng, Å., and Ellis, S.: Fracture and Weakening of Jammed Subduction Shear Zones, Leading to the Generation of Slow Slip Events, *Geochemistry, Geophysics, Geosystems*, 20, 4869–4884, <https://doi.org/10.1029/2019GC008481>, 2019.
- Bürgmann, R.: The geophysics, geology and mechanics of slow fault slip, *Earth and Planetary Science Letters*, 495, 112–134, <https://doi.org/10.1016/j.epsl.2018.04.062>, 2018.
- Carter, K. and Dworkin, S.: Channelized fluid flow through shear zones during fluid-enhanced dynamic recrystallization, Northern Apennines, Italy, *Geology*, 18, 720–723, [https://doi.org/10.1130/0091-7613\(1990\)018<0720:CFFTSZ>2.3.CO;2](https://doi.org/10.1130/0091-7613(1990)018<0720:CFFTSZ>2.3.CO;2), 1990.
- 470 Chen, J., Verberne, B., and Niemeijer, A.: Flow-to-Friction Transition in Simulated Calcite Gouge: Experiments and Microphysical Modelling, *Journal of Geophysical Research: Solid Earth*, p. e2020JB019970, <https://doi.org/10.1029/2020JB019970>, 2020.
- Cherukuri, H. and Shawki, T.: An energy-based localization theory: I. Basic framework, *International Journal of Plasticity*, 11, 15–40, [https://doi.org/10.1016/0749-6419\(94\)00037-9](https://doi.org/10.1016/0749-6419(94)00037-9), 1995.
- 475 Covey-crump, S.: The high temperature static recovery and recrystallization behaviour of cold-worked Carrara marble, *Journal of Structural Geology*, 19, 225–241, [https://doi.org/10.1016/S0191-8141\(96\)00088-0](https://doi.org/10.1016/S0191-8141(96)00088-0), 1997.
- Delle Piane, C., Burlini, L., Kunze, K., Brack, P., and Burg, J.-P.: Rheology of dolomite: Large strain torsion experiments and natural examples, *Journal of Structural Geology*, 30, 767–776, <https://doi.org/10.1016/j.jsg.2008.02.018>, 2008.
- Dimanov, A., Rybacki, E., Wirth, R., and Dresen, G.: Creep and strain-dependent microstructures of synthetic anorthite-diopside aggregates, *Journal of Structural Geology*, 29, 1049–1069, <https://doi.org/10.1016/j.jsg.2007.02.010>, 2007.
- 480 Edmond, J. and Paterson, M.: Volume changes during the deformation of rocks at high pressures, *International Journal of Rock Mechanics and Mining Sciences & Geomechanics Abstracts*, 9, 161–182, [https://doi.org/10.1016/0148-9062\(72\)90019-8](https://doi.org/10.1016/0148-9062(72)90019-8), 1972.
- Egholm, D., Knudsen, M., Clark, C., and Lesemann, J.: Modeling the flow of glaciers in steep terrains: The integrated second-order shallow ice approximation (iSOSIA), *Journal of Geophysical Research: Earth Surface*, 116, <https://doi.org/10.1029/2010JF001900>, 2011.
- 485 Evans, B.: Creep constitutive laws for rocks with evolving structure, *Geological Society, London, Special Publications*, 245, 329–346, <https://doi.org/10.1144/GSL.SP.2005.245.01.16>, 2005.
- Fossen, H. and Cavalcante, G.: Shear zones - A review, *Earth-Science Reviews*, 171, 434–455, <https://doi.org/10.1016/j.earscirev.2017.05.002>, 2017.
- Fressengeas, C. and Molinari, A.: Instability and localization of plastic flow in shear at high strain rates, *Journal of the Mechanics and Physics of Solids*, 35, 185–211, [https://doi.org/10.1016/0022-5096\(87\)90035-4](https://doi.org/10.1016/0022-5096(87)90035-4), 1987.
- 490 Fousseis, F., Regenauer-Lieb, K., Liu, J., Hough, R., and De Carlo, F.: Creep cavitation can establish a dynamic granular fluid pump in ductile shear zones, *Nature*, 459, 974–977, <https://doi.org/10.1038/nature08051>, 2009.

- Gilgannon, J., Fousseis, F., Menegon, L., Regenauer-Lieb, K., and Buckman, J.: Hierarchical creep cavity formation in an ultramylonite and implications for phase mixing, *Solid Earth*, 8, 1193–1209, <https://doi.org/10.5194/se-8-1193-2017>, 2017.
- 495 Gilgannon, J., Poulet, T., Berger, A., Barnhoorn, A., and Herwegh, M.: Dynamic recrystallisation can produce porosity in shear zones, *Geophysical Research Letters*, 47, e2019GL086172, <https://doi.org/10.1029/2019GL086172>, 2020.
- Giuntoli, F., Brovarone, A., and Menegon, L.: Feedback between high-pressure genesis of abiogenic methane and strain localization in subducted carbonate rocks, *Scientific reports*, 10, 1–15, <https://doi.org/10.1038/s41598-020-66640-3>, 2020.
- Goncalves, P., Poilvet, J.-C., Oliot, E., Trap, P., and Marquer, D.: How does shear zone nucleate? An example from the Suretta nappe (Swiss Eastern Alps), *Journal of Structural Geology*, 86, 166–180, <https://doi.org/10.1016/j.jsg.2016.02.015>, 2016.
- 500 Guével, A., Rattez, H., Alevizos, S., and Veveakis, M.: Contact phase-field modeling for chemo-mechanical degradation processes. Part I: Theoretical foundations, 2019.
- Haertel, M., Herwegh, M., and Pettke, T.: Titanium-in-quartz thermometry on synkinematic quartz veins in a retrograde crustal-scale normal fault zone, *Tectonophysics*, 608, 468–481, <https://doi.org/10.1016/j.tecto.2013.08.042>, 2013.
- 505 Handy, H., Hirth, G., and Bürgmann, R.: *Continental Fault Structure and Rheology from the Frictional-to-Viscous Transition Downward*, chap. 6, pp. 139–182, MIT Press, 2007.
- Hansen, L., Zimmerman, M., Dillman, A., and Kohlstedt, D.: Strain localization in olivine aggregates at high temperature: A laboratory comparison of constant-strain-rate and constant-stress boundary conditions, *Earth and Planetary Science Letters*, 333–334, 134–145, <https://doi.org/10.1016/j.epsl.2012.04.016>, 2012.
- 510 Herwegh, M. and Jenni, A.: Granular flow in polymineralic rocks bearing sheet silicates: new evidence from natural examples, *Tectonophysics*, 332, 309 – 320, [https://doi.org/10.1016/S0040-1951\(00\)00288-2](https://doi.org/10.1016/S0040-1951(00)00288-2), 2001.
- Herwegh, M. and Kunze, K.: The influence of nano-scale second-phase particles on deformation of fine grained calcite mylonites, *Journal of Structural Geology*, 24, 1463–1478, [https://doi.org/10.1016/S0191-8141\(01\)00144-4](https://doi.org/10.1016/S0191-8141(01)00144-4), 2002.
- Herwegh, M., de Bresser, J., and ter Heege, J.: Combining natural microstructures with composite flow laws: an improved approach for the 515 extrapolation of lab data to nature, *Journal of Structural Geology*, 27, 503–521, <https://doi.org/10.1016/j.jsg.2004.10.010>, 2005.
- Hobbs, B. and Ord, A.: *Structural Geology: The Mechanics of Deforming Metamorphic Rocks*, Elsevier, Netherlands, 2015.
- Hobbs, B., Ord, A., and Teysier, C.: Earthquakes in the ductile regime?, *Pure and Applied Geophysics*, 124, 309–336, <https://doi.org/10.1007/BF00875730>, 1986.
- Kocks, U., Argon, A., and Ashby, M.: Thermodynamics and kinetics of slip, vol. 19 of *Progress in Materials Science*, Pergamon Press Ltd, 520 1975.
- Lopez-Sanchez, M. A. and Llana-Fúnez, S.: A cavitation-seal mechanism for ultramylonite formation in quartzofeldspathic rocks within the semi-brittle field (Vivero fault, NW Spain), *Tectonophysics*, 745, 132–153, <https://doi.org/10.1016/j.tecto.2018.07.026>, 2018.
- Mariani, E., Brodie, K., and Rutter, E.: Experimental deformation of muscovite shear zones at high temperatures under hydrothermal conditions and the strength of phyllosilicate-bearing faults in nature, *Journal of Structural Geology*, 28, 1569–1587, 525 <https://doi.org/10.1016/j.jsg.2006.06.009>, 2006.
- Menegon, L., Fousseis, F., Stünitz, H., and Xiao, X.: Creep cavitation bands control porosity and fluid flow in lower crustal shear zones, *Geology*, 43, 227–230, <https://doi.org/10.1130/G36307.1>, 2015.
- Neupauer, R. and Powell, K.: A fully-anisotropic Morlet wavelet to identify dominant orientations in a porous medium, *Computers & Geosciences*, 31, 465–471, <https://doi.org/10.1016/j.cageo.2004.10.014>, 2005.

- 530 Neupauer, R., Powell, K., Qi, X., Lee, D., and Villhauer, D.: Characterization of permeability anisotropy using wavelet analysis, *Water Resources Research*, 42, <https://doi.org/10.1029/2005WR004364>, 2006.
- Noack, L. and Breuer, D.: Plate tectonics on rocky exoplanets: Influence of initial conditions and mantle rheology, *Planetary and Space Science*, 98, 41–49, <https://doi.org/10.1016/j.pss.2013.06.020>, 2014.
- Paterson, M.: Localization in rate-dependent shearing deformation, with application to torsion testing, *Tectonophysics*, 445, 273–280, 535 <https://doi.org/10.1016/j.tecto.2007.08.015>, 2007.
- Peacock, S.: Thermal and metamorphic environment of subduction zone episodic tremor and slip, *Journal of Geophysical Research: Solid Earth*, 114, <https://doi.org/10.1029/2008JB005978>, 2009.
- Peters, M., Herwegh, M., Paesold, M., Poulet, T., Regenauer-Lieb, K., and Veveakis, M.: Boudinage and folding as an energy instability in ductile deformation, *Journal of Geophysical Research: Solid Earth*, 121, 3996–4013, <https://doi.org/10.1002/2016JB012801>, 2016.
- 540 Pieri, M., Kunze, K., Burlini, L., Stretton, I., Olgaard, D., Burg, J.-P., and Wenk, H.-R.: Texture development of calcite by deformation and dynamic recrystallization at 1000K during torsion experiments of marble to large strains, *Tectonophysics*, 330, 119–140, [https://doi.org/10.1016/S0040-1951\(00\)00225-0](https://doi.org/10.1016/S0040-1951(00)00225-0), 2001.
- Poirier, J.-P.: *Creep of Crystals: High-Temperature Deformation Processes in Metals, Ceramics and Minerals*, Cambridge Earth Science Series, Cambridge University Press, <https://doi.org/10.1017/CBO9780511564451>, 1985.
- 545 Poulet, T., Veveakis, M., Herwegh, M., Buckingham, T., and Regenauer-Lieb, K.: Modeling episodic fluid-release events in the ductile carbonates of the Glarus thrust, *Geophysical Research Letters*, 41, 7121–7128, <https://doi.org/10.1002/2014GL061715>, 2014.
- Préçigout, J., Prigent, C., Palasse, L., and Pochon, A.: Water pumping in mantle shear zones, *Nature Communications*, 8, 15 736, <https://doi.org/10.1038/ncomms15736>, 2017.
- Préçigout, J., Stünitz, H., and Villeneuve, J.: Excess water storage induced by viscous strain localization during high-pressure shear experiment, *Scientific Reports*, 9, 3463, <https://doi.org/10.1038/s41598-019-40020-y>, 2019. 550
- Regenauer-Lieb, K., Yuen, D., and Fousseis, F.: Landslides, Ice Quakes, Earthquakes: A Thermodynamic Approach to Surface Instabilities, pp. 1885–1908, https://doi.org/10.1007/978-3-0346-0138-2_15, 2009.
- Regenauer-Lieb, K., Veveakis, M., Poulet, T., Paesold, M., Rosenbaum, G., Weinberg, R., and Karrech, A.: Multiscale, multiphysics geomechanics for geodynamics applied to buckling instabilities in the middle of the Australian craton, *Philosophical Magazine*, 95, 3055–3077, 555 <https://doi.org/10.1080/14786435.2015.1066517>, 2015.
- Renner, J. and Evans, B.: Do calcite rocks obey the power-law creep equation?, *Geological Society, London, Special Publications*, 200, 293–307, <https://doi.org/10.1144/GSL.SP.2001.200.01.17>, 2002.
- Rybacki, E., Wirth, R., and Dresen, G.: High-strain creep of feldspar rocks: Implications for cavitation and ductile failure in the lower crust, *Geophysical Research Letters*, 35, <https://doi.org/10.1029/2007GL032478>, 2008.
- 560 Rybacki, E., Wirth, R., and Dresen, G.: Superplasticity and ductile fracture of synthetic feldspar deformed to large strain, *Journal of Geophysical Research: Solid Earth*, 115, <https://doi.org/10.1029/2009JB007203>, 2010.
- Schmid, S. and Handy, M.: Towards a genetic classification of fault rocks - geological usage and tectonophysical implications, chap. 16, pp. 339–361, Academic Press, New York, 1991.
- Selverstone, J., Morteani, G., and Staude, J.-M.: Fluid channelling during ductile shearing: transformation of granodiorite into aluminous schist in the Tauern Window, Eastern Alps, *Journal of Metamorphic Geology*, 9, 419–431, <https://doi.org/10.1111/j.1525-1314.1991.tb00536.x>, 1991. 565

- Shawki, T.: An Energy Criterion for the Onset of Shear Localization in Thermal Viscoplastic Materials, Part II: Applications and Implications., *Journal of Applied Mechanics*, 61, 538–547, <https://doi.org/10.1115/1.2901493>, 1994.
- 570 Shigematsu, N., Fujimoto, K., Ohtani, T., and Goto, K.: Ductile fracture of fine-grained plagioclase in the brittle-plastic transition regime: implication for earthquake source nucleation, *Earth and Planetary Science Letters*, 222, 1007–1022, <https://doi.org/10.1016/j.epsl.2004.04.001>, 2004.
- Sibson, R.: Fault rocks and fault mechanisms, *Journal of the Geological Society*, 133, 191–213, <https://doi.org/10.1144/gsjgs.133.3.0191>, 1977.
- 575 Sibson, R.: Crustal stress, faulting and fluid flow, Geological Society, London, Special Publications, 78, 69–84, <https://doi.org/10.1144/GSL.SP.1994.078.01.07>, 1994.
- Spiess, R., Dibona, R., Rybacki, E., Wirth, R., and Dresen, G.: Depressurized Cavities within High-strain Shear Zones: their Role in the Segregation and Flow of SiO₂-rich Melt in Feldspar-dominated Rocks, *Journal of Petrology*, 53, 1767–1776, <https://doi.org/10.1093/petrology/egs032>, 2012.
- 580 Tannock, L., Herwegh, M., Berger, A., Liu, J., and Regenauer-Lieb, K.: The effects of a tectonic stress regime change on crustal-scale fluid flow at the Heyuan geothermal fault system, South China, *Tectonophysics*, 781, 228–399, <https://doi.org/10.1016/j.tecto.2020.228399>, 2020.
- Torrence, C. and Compo, G.: A Practical Guide to Wavelet Analysis, *Bulletin of the American Meteorological Society*, 79, 61–78, [https://doi.org/10.1175/1520-0477\(1998\)079<0061:APGTWA>2.0.CO;2](https://doi.org/10.1175/1520-0477(1998)079<0061:APGTWA>2.0.CO;2), 1998.
- 585 van der Walt, S., Schönberger, J., Nunez-Iglesias, J., Boulogne, F., Warner, J., Yager, N., Gouillart, E., Yu, T., and the scikit-image contributors: scikit-image: image processing in Python, *PeerJ*, 2, e453, <https://doi.org/10.7717/peerj.453>, 2014.
- Vauchez, A., Tommasi, A., and Mainprice, D.: Faults (shear zones) in the Earth's mantle, *Tectonophysics*, 558–559, 1–27, <https://doi.org/10.1016/j.tecto.2012.06.006>, 2012.
- 590 Verberne, B., Chen, J., Niemeijer, A., de Bresser, J., Pennock, G., Drury, M., and Spiers, C.: Microscale cavitation as a mechanism for nucleating earthquakes at the base of the seismogenic zone, *Nature Communications*, 8, 1645, <https://doi.org/10.1038/s41467-017-01843-3>, 2017.
- Veveakis, E. and Regenauer-Lieb, K.: Review of extremum postulates, *Current Opinion in Chemical Engineering*, 7, 40–46, <https://doi.org/10.1016/j.coche.2014.10.006>, 2015.
- Wang, K. and Tréhu, A.: Invited review paper: Some outstanding issues in the study of great megathrust earthquakes - The Cascadia example, *Journal of Geodynamics*, 98, 1–18, <https://doi.org/10.1016/j.jog.2016.03.010>, 2016.
- 595 Weinberg, R. and Regenauer-Lieb, K.: Ductile fractures and magma migration from source, *Geology*, 38, 363–366, <https://doi.org/10.1130/G30482.1>, 2010.
- Xiao, X., Evans, B., and Bernabé, Y.: Permeability Evolution During Non-linear Viscous Creep of Calcite Rocks, pp. 2071–2102, Birkhäuser Basel, Basel, https://doi.org/10.1007/978-3-7643-8124-0_3, 2006.
- 600 Závada, P., Schulmann, K., Konopásek, J., Stanislav, U., and Ondrej, L.: Extreme ductility of feldspar aggregates - Melt-enhanced grain boundary sliding and creep failure: Rheological implications for felsic lower crust, *Journal of Geophysical Research: Solid Earth*, 112, <https://doi.org/10.1029/2006JB004820>, 2007.